DOI: 10.1002/cmdc.201100522

Chiral Mercaptoacetamides Display Enantioselective Inhibition of Histone Deacetylase 6 and Exhibit Neuroprotection in Cortical Neuron Models of Oxidative Stress

Jay H. Kalin,[a] Hankun Zhang,[a] Sophie Gaudrel-Grosay,[a] Giulio Vistoli,[b] and Alan P. Kozikowski*[a]

Mercaptoacetamide-based ligands have been designed as a new class of histone deacetylase (HDAC) inhibitors for possible use in the treatment of neurodegenerative diseases. The thiol group of these compounds provides a key binding element for interaction with the catalytic zinc ion, and thus differs from the more typically employed hydroxamic acid based zinc binding groups. Herein we disclose the chemistry and biology of some substituted mercaptoacetamides with the intention of increasing HDAC6 isoform selectivity while maintaining potency similar to their hydroxamic acid analogues. The introduction of a stereocenter α to the thiol group was found to have a considerable impact on HDAC inhibitor potency. These new compounds were also profiled for their therapeutic potential in an in vitro model of stress-induced neuronal injury and were found to act as nontoxic neuroprotective agents.

Introduction

Histone deacetylases (HDACs) are implicated in the epigenetic regulation of gene expression via chromatin modification. A condensed, transcriptionally silent chromatin structure is obtained when the anionic phosphate groups of the DNA backbone interact with the cationic lysine residues of histone proteins. Histone deacetylases are part of this process, facilitating these ionic interactions by removing *N*-acetyllysine residues from nucleosomal histone tails. Moreover, HDACs accept a variety of non-histone substrates such as transcription factors and regulators, as well as structural and chaperone proteins.[1–4] It is this latter mechanism by which selective HDAC6 inhibitors are believed to exert their neuroprotective properties, as HDAC6 inhibition has been linked to upregulation of the transport of brain-derived neurotrophic factor (BDNF), a protein involved in neurogenesis, mediation of peroxiredoxins, an important class of redox regulators, and regulation of Hsp90, an important chaperone protein involved in a number of cell signaling processes.[4–7] Additionally, HDAC6-selective inhibitors have been suggested to lack some of the major side effects associated with broad-spectrum histone deacetylase inhibitors (HDACIs).[8–10] Thus, our particular interest has focused on HDAC6, which is highly expressed in the brain and therefore serves an additional role in controlling gene transcription in neurons.[11]

The development of selective HDACIs has emerged as a challenging field in drug discovery, as many of the residues involved in substrate recognition and catalytic activity are conserved across the HDAC isoforms.[12,13] Only a few HDAC6-selective inhibitors are known; they are of great interest, not only as tools for probing the biological functions of the isoform, but also as possible therapeutic agents with few side effects.[10,14] Many known HDACIs such as suberoylanilide hydroxamic acid (SAHA) and trichostatin A (TSA) contain a hydroxamic acid zinc binding group (ZBG); however, in addition to being metabolically labile (orally administered SAHA has a half-life of 1.5–2 h in humans), hydroxamates are very potent metal-chelating agents that could lead to off-target activity at other zinc-containing enzymes such as matrix metalloproteases, MMP-1, MMP-2, and MMP-3, ultimately resulting in undesirable toxicity (Supporting Information figure 1).[10,15–18] In neuronal models of oxidative stress, many hydroxamic acid based HDACIs were found to exhibit some intrinsic toxicity, whereas their mercaptoacetamide counterparts were found to be fully neuroprotective, suggesting that alternative ZBGs may be preferred depending on the desired therapeutic goal.[15,19–21] However, examples of neuroprotective hydroxamic acid HDACIs have also been identified.[15]

Previously we reported on the synthesis of a series of mercaptoacetamide-based HDACIs that exhibit some HDAC6 selectivity and were found to have better therapeutic profiles in protecting neurons against oxidative stress-induced cell death

[a] *J. H. Kalin,[+] Dr. H. Zhang,[+] Dr. S. Gaudrel-Grosay, Prof. A. P. Kozikowski*
Department of Medicinal Chemistry and Pharmacognosy
University of Illinois at Chicago
833 S. Wood Street, Chicago, IL 60612-7211 (USA)
E-mail: kozikowa@uic.edu

[b] *Dr. G. Vistoli*
Dipartimento di Scienze Farmaceutiche "Pietro Pratesi"
Università degli Studi di Milano, Via Mangiagalli 25, 20133, Milan (Italy)

[+] *These authors contributed equally to this work.*

Supporting information for this article is available on the WWW under http://dx.doi.org/10.1002/cmdc.201100522.

 © 2012 Wiley-VCH Verlag GmbH & Co. KGaA, Weinheim

relative to their hydroxamic acid homologues.[15] The mechanism of HDAC inhibition by mercaptoacetamide-based HDACIs is, theoretically, similar to that of the hydroxamates, in that both have the potential to chelate zinc in a monodentate or bidentate fashion depending on the isoform.[13,22] In addition to our previously reported analogues, numerous examples of thiol-containing HDACIs have been reported.[10,22,23] However, one potential drawback of these mercaptoacetamide HDACIs is their ability to undergo oxidative dimerization to the disulfide. Although this disulfide bond can be reduced within cells to afford the parent monomers, it can present a problem when profiling the activity of these inhibitors against purified proteins.[24] Thus, we synthesized a novel series of modestly potent mercaptoacetamide-based HDAC6-selective inhibitors that display increased resistance to dimerization, and evaluated their ability to protect primary cortical neurons from oxidative stress-induced cell death.

Results and Discussion

Chemistry

The synthetic procedures used for the preparation of our first series of amide-linked mercaptoacetamide isoxazoles are outlined in Scheme 1. Here, a nitrile oxide cycloaddition was employed to generate the trisubstituted isoxazole **1** starting from (*E*)-benzaldehyde chloro-oxime and ethyl-2-butynoate using microwave irradiation. This ester was saponified to yield acid **2** and then allowed to react with a diamine linker in the presence of the coupling agent PyBOP to yield **3**. The Boc protecting group was removed to give amine **4**, and then a second coupling reaction was carried out with different trityl- or pivaloyl-protected mercaptoacetic acids **5a**–**d**. The pivaloyl-protected prodrug **6d** was thus made available for study. The trityl group was removed from compounds **6a**–**6c** to afford three mercaptoacetamide ligands with no (**7a**), one (**7b**), or two (**7c**) methyl groups α to the thiol of the mercaptoacetamide.

Because it is well known that the absolute stereochemistry of a particular molecule can greatly influence its activity, we also chose to investigate the individual enantiomers of compound **7b**. The enantiomers of compound **6b** were separated by chiral column chromatography and then deprotected to afford the single enantiomers, (*R*)-**7b** and (*S*)-**7b** (Scheme 2). To determine the absolute stereochemistry of the two isolated enantiomers, starting from (*S*)-2-aminopropanoic acid and **4**, we synthesized the *R* isomer of compound **6b** and compared the retention time of the pure enantiomer to that of the racemic mixture; we then observed that the *R* isomer was the first to elute from the column (Supporting Information scheme 1 and figure 2).[25]

As we were aware of the fact that the hydroxamic acid group may be associated with neuronal toxicity, we synthesized an analogue to compare it with our mercaptoacetamide-based ligands both in terms of potency and neuroprotective properties (Scheme 3). The hydroxamic acid **9** was prepared in two steps from the isoxazole acid **2** using standard PyBOP coupling protocol and then hydroxyamine to supplant the obtained methyl ester.

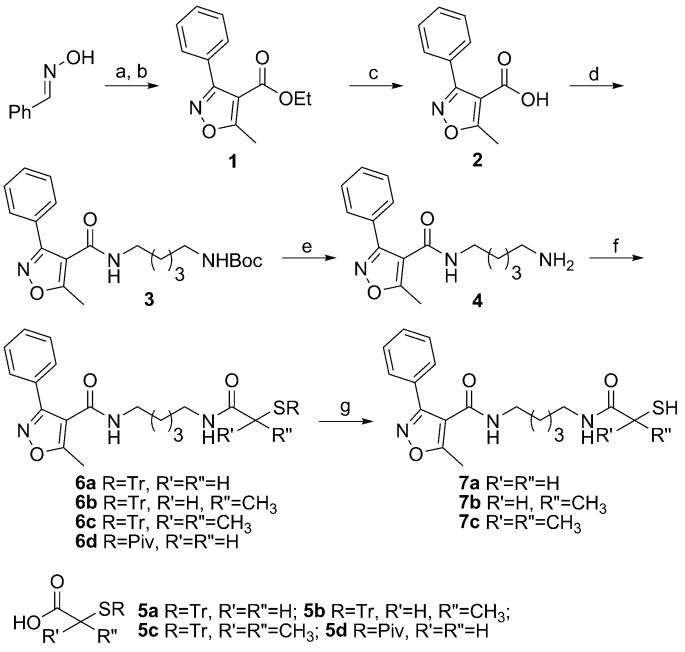

Scheme 1. *Reagents and conditions*: a) *N*-chlorosuccinimide, Al_2O_3, microwave, 40 °C; b) ethyl-2-butynoate, Et_3N, THF, microwave, 70 °C; c) NaOH, CH_3OH/H_2O, 60 °C; d) NH_2-$(CH_2)_5$NHBoc, PyBOP, DIEA, CH_2Cl_2, RT; e) TFA, CH_2Cl_2, RT; f) **5**, PyBOP, DIEA, CH_2Cl_2, RT; g) TFA, Et_3SiH, CH_2Cl_2, 0 °C→RT.

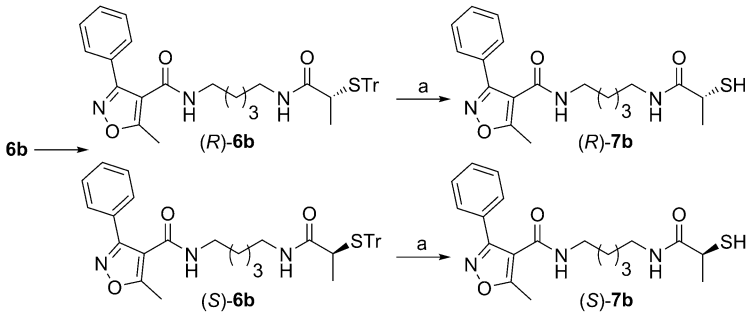

Scheme 2. *Reagents and conditions*: a) TFA, Et_3SiH, CH_2Cl_2, 0 °C→RT.

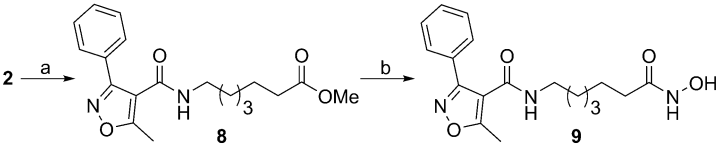

Scheme 3. *Reagents and conditions*: a) $NH_2(CH_2)_6CO_2Me$·HCl, PyBOP, DIEA, CH_2Cl_2, RT; b) NH_2OH·HCl, KOH, CH_3OH, RT.

 © 2012 Wiley-VCH Verlag GmbH & Co. KGaA, Weinheim

As shown in Scheme 4, the synthesis of alkene-linked mercaptoacetamides **13a–d** was performed in 5 or 6 steps starting from the previously obtained acid **2**. Compound **2** was reduced to the alcohol and subsequently oxidized to aldehyde **11**. A Wittig reaction was then employed with aldehyde **11**

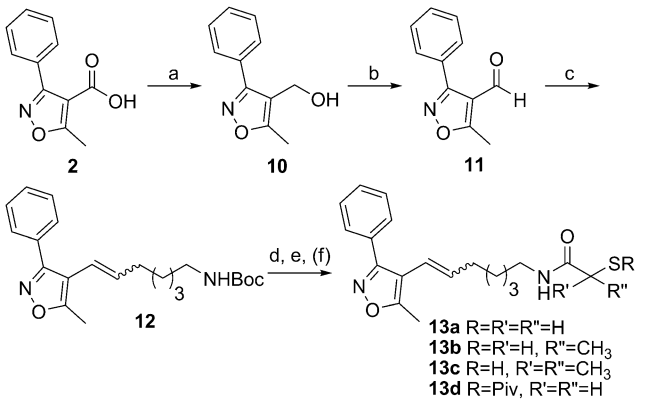

Scheme 4. *Reagents and conditions*: a) Borane-THF, THF, 0 °C→RT; b) MnO_2, CH_2Cl_2, RT; c) $BrPh_3P(CH_2)_6NHBoc$, *n*BuLi, THF, 0 °C→RT; d) TFA, CH_2Cl_2, RT; e) **5**, PyBOP, DIEA, CH_2Cl_2, RT; f) TFA, Et_3SiH, CH_2Cl_2, 0 °C→RT.

and a prepared phosphonium salt to produce compound **12**. Procedures similar to those described in Scheme 1 were applied to compound **12** to generate the α-unsubstituted, mono-, and dimethylmercaptoacetamides. To investigate the difference in activity between the geometric isomers generated during the Wittig reaction, the isomers of compounds **13a** and **13d** were isolated by chiral column chromatography, and their molecular configuration was assigned based on ^{1}H NMR (Supporting Information scheme 2 and figure 3).

Ligand **16**, the compound containing an ether linker, was synthesized from alcohol **10** by conversion into the iodo precursor via an Appel-like reaction. This was subsequently allowed to react with Boc-aminopentanol to yield intermediate carbamate **14**. The obtained product was transformed as previously described in Scheme 1 into the desired α-methylmercaptoacetamide (Scheme 5). Again, to investigate the effect of stereochemistry on compound activity, the enantiomers of compound **15** were isolated by chiral column chromatography and then deprotected to yield (*R*)-**16** and (*S*)-**16** (Supporting Information scheme 3). The absolute stereochemistry was assigned in the same manner as that for compound **7b** (Supporting Information scheme 4 and figure 4).

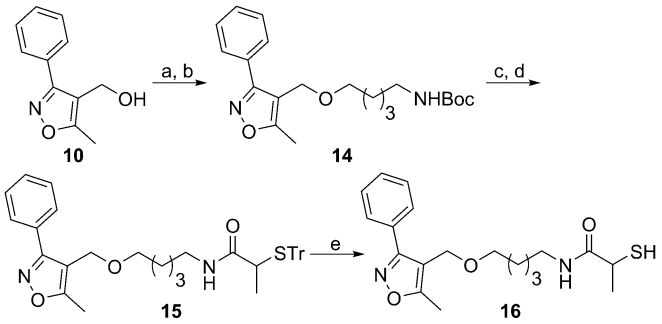

Scheme 5. *Reagents and conditions*: a) I_2, PPh_3, imidazole, CH_2Cl_2, 0 °C→RT; b) $HO(CH_2)_5NHBoc$, NaH, DMF, −20 °C→RT; c) TFA, CH_2Cl_2, RT; d) **5b**, PyBOP, DIEA, CH_2Cl_2, RT; e) TFA, Et_3SiH, CH_2Cl_2, 0 °C→RT.

Synthesis of the alkyne- and cinnamoyl-linked mercaptoacetamides was performed by starting from commercially available or readily obtained iodoisoxazoles **17a–b**. The Sonogashira and Heck reactions, followed by conditions similar to those described in Scheme 1, were used with **17a–b** to generate the alkyne- and cinnamoyl-linked compounds **18a–e** and **20a–b**, respectively (Scheme 6). With the desired compounds in hand, we next studied their activity in both the isolated enzyme assays and in cell-based neuroprotection studies.

HDAC isoform inhibition

IC_{50} values were determined for these new mercaptoacetamide ligands at selected HDAC isoforms using a fluorescence-based assay, and the results are listed in Table 1. Mercaptoacetamide **7a** showed sub-micromolar HDAC6 activity with some selectivity over both the class I (> 21-fold) and class IIa (> 38-fold) isozymes. The related hydroxamic acid **9** exhibited similar activity and selectivity at the class I and class IIa isoforms (> 14- and

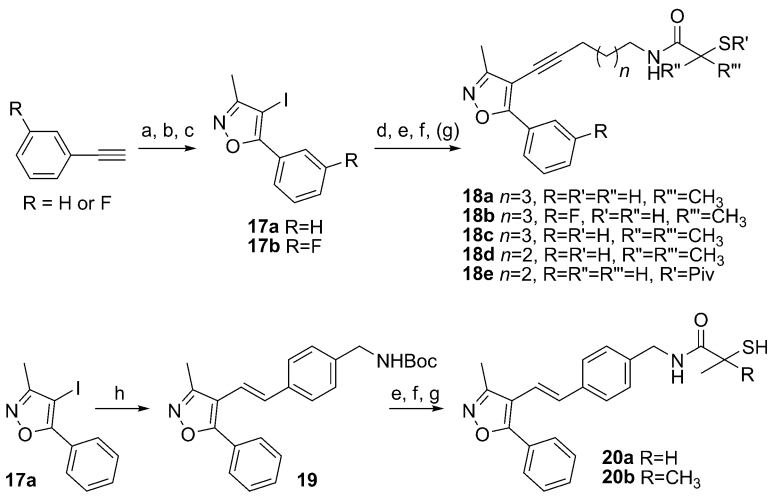

Scheme 6. *Reagents and conditions*: a) $ClCOCH_3$, $ZnCl_2$, *n*BuLi, THF, −78 °C; b) $NH_2OMe{\cdot}HCl$, pyridine, Na_2SO_4, CH_3OH, reflux; c) ICl, CH_2Cl_2, reflux; d) $HCC(CH_2)_nNHBoc$, $PdCl_2(PPh_3)_2$, CuI, DIEA, DMF, microwave, 130 °C; e) TFA, CH_2Cl_2, RT; f) **5**, PyBOP, DIEA, CH_2Cl_2, RT; g) TFA, Et_3SiH, CH_2Cl_2, 0 °C→RT; h) *tert*-butyl 4-vinylbenzylcarbamate, $Pd(OAc)_2$, nBu_4NCl, Na_2CO_3, DMF, microwave, 130 °C.

 © 2012 Wiley-VCH Verlag GmbH & Co. KGaA, Weinheim

Table 1. In vitro HDAC isoform inhibitory activity.[a]

Compd	Class I			Class IIa		Class IIb
	HDAC1	HDAC2	HDAC3	HDAC4	HDAC5	HDAC6
6d	–	–	–	–	–	–
7a	5.7 ± 0.5[e]	28	14	10	15	0.26 ± 0.03[e]
7b[b]	>30	>30	>30	>30	>30	1.1 ± 0.01[e]
(*R*)-**7b**	>30[e]	>30[e]	15 ± 1[e]	>30[e]	>30[e]	0.28 ± 0.04[e]
(*S*)-**7b**	>30[e]	>30[e]	>30[e]	>30[e]	>30[e]	>30[e]
7c	>30	>30	>30	>30	>30	>30
9	3.0 ± 0.2[e]	11	2.6	9.4	6.0	0.18 ± 0.08[e]
13a[c]	>30	>30	>30	>30	>30	2.7 ± 0.1[e,f]
cis-**13a**	>30[e]	–	–	>30[e]	–	4.8 ± 1.8[e,f]
trans-**13a**	28 ± 4[e]	–	–	>30[e]	–	3.5 ± 0.5[e,f]
13b[b,c]	>30	>30	>30	>30	>30	9.8
13c[c]	>30	>30	>30	>30	>30	>30
13d[c]	>30	>30	>30	>30	>30	>30[e]
cis-**13d**	>30	–	–	–	–	>30[e]
trans-**13d**	>30	–	–	–	–	>30[e]
16[b]	9.6	14	5.5	>30	>30	0.85
(*R*)-**16**	1.5 ± 0.03[e]	–	3.4 ± 0.2[e]	–	–	0.83 ± 0.27[e]
(*S*)-**16**	>30[e]	–	>30[e]	–	–	>30[e]
18a[b]	2.7	7.5	1.4	>30	8.3	2.0
18b[b]	3.7	9.4	2.1	>30	13	2.6
18c	>30	>30	>30	>30	>30	>30
18d	>30	>30	>30	>30	>30	>30
18e	–	–	–	–	–	–
20a[b]	>30	>30	>30	>30	>30	>30
20b	>30	>30	>30	>30	>30	>30
TSA[d]	0.006 ± 0.003	0.017 ± 0.008	0.008 ± 0.004	0.047 ± 0.061	0.013 ± 0.007	0.0017 ± 0.0005

[a] These results were determined by CRO Reaction Biology (Malvern, PA, USA); ten-dose IC_{50} values were determined by using threefold serial dilutions starting at concentrations of 30 μM. Compounds with $IC_{50} > 30$ μM were considered to be inactive. A dashed line indicates that the compound was not tested at that isoform. [b] Racemic mixture. [c] Mixture of geometric isomers. [d] IC_{50} values for TSA are reported as the average of five experiments ± SD for HDAC1, 3, 4, and 6, and the average of four experiments ± SD for HDAC2 and 5. [e] Evaluated in duplicate. [f] $p > 0.05$ (difference not statistically significant), determined using the unpaired *t*-test available in GraphPad Prism 5 (La Jolla, CA, USA).

>33-fold, respectively). The slight difference in potency observed between **7a** and **9** may result from the ability of **9** to form an additional hydrogen bond to the enzyme. It is known that the NH group of the hydroxamate ZBG is able to form a hydrogen bond with a histidine residue in the HDAC active site, whereas the mercaptoacetamide ZBG lacks this functionality.[26] The addition of a methyl group to the mercaptoacetamide ZBG of **7a**, compound **7b**, resulted in a slight decrease in potency (**7a** $IC_{50} = 0.26$ μM, **7b** $IC_{50} = 1.1$ μM); however, the activity at all other HDAC isoforms was abolished. Because **7b** was a racemic mixture, we isolated the single enantiomers and observed that the *R* isomer displays sub-micromolar activity at HDAC6, similar to the original unsubstituted compound **7a**, whereas (*S*)-**7b** is completely inactive. Compound (*R*)-**7b** maintained selectivity over all the other HDAC isoforms except HDAC3, for which the ten-dose IC_{50} was found to be 15 μM.

Additional modifications were made to the linker region and cap group of these mercaptoacetamides. Replacing the amide linker of **7a** by an alkene, **13a**, resulted in micromolar HDAC6 activity and a good selectivity profile, with the IC_{50} at all other tested isoforms being >30 μM. To investigate the effect of geometric isomerism on compound activity, the isomers of **13a**—*cis*- and *trans*-**13a**—were isolated and found to exhibit similar activity at HDAC6 and a less than twofold difference in activity at HDAC1, suggesting that the geometric configuration of the double bond at this position in the linker has little effect on ligand binding. The pivaloyl prodrug of **13a**, compound **13d**, along with the individual geometric isomers, *cis*-**13d** and *trans*-**13d**, displayed no inhibition at any of the HDAC isoforms tested. This was expected, as these IC_{50} values were measured using purified protein; as such, no metabolic enzymes were present to release the active form of the drug.[27] The other pivaloyl prodrugs, **6d** and **18e**, were not screened against the isolated HDAC enzymes for this reason.

With an ether linker replacing the amide, as in compound **16**, HDAC6 activity was still observed in the sub-micromolar range, and selectivity over the class I (>6-fold) and class IIa (>35-fold) isoforms was similar to that of compound **7a**. Again, we investigated the effect of absolute stereochemistry on compound activity and found that the *R* isomer of **16** exhibits HDAC6 activity in the sub-micromolar range, whereas (*S*)-**16** is completely inactive. These results combined with the results obtained for the enantiomers of compound **7b** led us to conclude that the *R* configuration of the monomethyl mercaptoacetamide ZBG is preferred for HDAC6 activity.

Lastly, the compounds containing alkyne linkers and monomethyl mercaptoacetamide ZBGs (**18a**–**b**) exhibited micromolar activity, with only some selectivity over the HDAC4 isoform. Compounds containing a cinnamoyl linker (**20a**–**b**) showed no HDAC activity, perhaps due to the rigidity of this linker. The ad-

 © 2012 Wiley-VCH Verlag GmbH & Co. KGaA, Weinheim

dition of two methyl groups to the ZBG, as with **18c** and **18d**, completely abolished activity at every tested HDAC isoform and for all cap group and linker modifications. This loss of activity can likely be attributed to steric interactions in the active site. Although the HDAC proteins are able to accommodate some steric bulk, the addition of a second methyl group likely renders the compound unable to adopt a conformation that does not clash with active site residues.

Molecular modeling

With the intent of rationalizing the stereoselectivity observed with the reported mercaptoacetamides, a molecular docking study was carried out considering the two enantiomers of **7b**, (*R*)-**7b** and (*S*)-**7b**, and three relevant HDAC subtypes. To minimize the number of exploited homology models, the following structures were studied: a) X-ray structure of the human HDAC2 isozyme (PDB ID: 3MAX) as representative of the class I subtypes; b) X-ray structure of the human HDAC4 isozyme (PDB ID: 2VQM) as representative of the class IIa subtypes; and c) homology model of the second catalytic domain of human HDAC6 (class IIb) as recently generated by us.[14] Given the high degree of sequence homology between HDAC1 and HDAC2, the results obtained for HDAC2 can be considered similar to what would be observed with HDAC1. The docking calculations were carried out considering the anionic form of the thiol for the two enantiomers. Also, the two His–Asp dyads that characterize the catalytic core of the HDAC isozymes were considered in their singly protonated state such that only the first histidine residue (His145 for HDAC2, His158 for HDAC4, and His610 for HDAC6-CDII) was protonated, while the second histidine residue (His146 for HDAC2, His159 for HDAC4, and His611 for HDAC6-CDII) was considered neutral and in its N^{ε} tautomeric form to minimize steric hindrance within the catalytic pocket. This choice was justified by considering the precise planarity that characterizes the first dyad and increases its basicity, whereas the other dyad does not show similar planarity, resulting in a less basic histidine residue. This is also in line with other enzymatic studies demonstrating that the first protonation highly disfavors a second protonation of His146, allowing facile proton transfer between the two dyads.[28]

The electrostatic energy scores, as determined with VEGA using a distance-dependent dielectric function, for all minimized complexes between HDAC isozymes and enantiomers (*R*)-**7b** and (*S*)-**7b** were lower for the *R* isomer than for the *S* isomer, confirming the observed stereoselectivity (Supporting Information table 1). The observed difference in binding mode for the two enantiomers can be explained by considering the interactions available to the amido group of each ligand (Figure 1a). Indeed, in both complexes, the sulfur atom approaches the zinc ion, which also interacts with protonated His145; however, only the amido group of the *R* isomer was able to interact with the zinc ion and stabilize hydrogen bonding interactions with the highly conserved Tyr308 residue. Conversely, the amido group of the *S* isomer was unable to elicit these significant interactions, and also clashes with Cys156. This is in line with recent mechanistic studies, which found

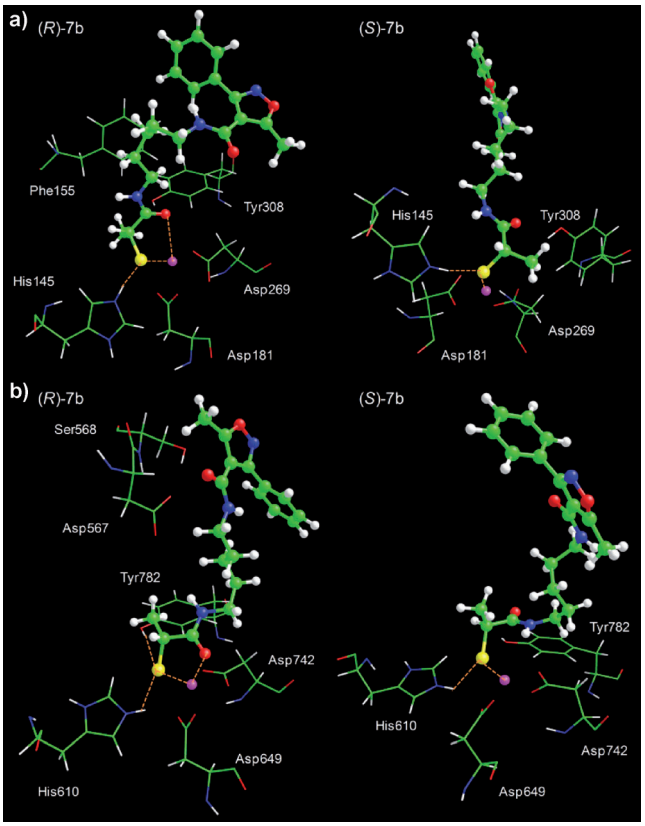

Figure 1. a) Putative complexes for (*R*)-**7b** and (*S*)-**7b** with the resolved HDAC2 crystal structure (PDB ID: 3MAX) illustrating that only the active *R* isomer can elicit bidentate chelation, which is reinforced by hydrogen bonding interactions between the amido group of the ligand and Tyr308. b) Putative complexes for the two enantiomers (*R*)-**7b** and (*S*)-**7b** with the second catalytic subunit of the HDAC6 subtype (previously published),[14] illustrating that only the active *R* isomer can elicit bidentate chelation reinforced by hydrogen bonding between the sulfur atom and Tyr782. This difference was also reflected by the position of the cap group, as only the active *R* isomer was able to stabilize hydrogen bonding interactions with Asp567 and Ser568 on the cavity rim.

that inhibitors of class I isozymes are characterized by a tight bidentate chelation with the zinc ion which is reinforced by a hydrogen bonding interaction with the conserved tyrosine residue and is not dependent on the ionization state of the inhibitor.[29] The differing arrangement of the ZBG moieties also reflect on the interactions stabilized by the cap group, such that the *R* isomer is able to assume a more folded geometry and can stabilize two relevant hydrogen bonds with His183 and Tyr209 in addition to a rich set of hydrophobic contacts, whereas the *S* isomer assumes a more extended conformation and does not display these interactions.

The role of the cap group moiety is even more preponderant in HDAC4 (complexes not shown) as the ZBG group realizes a similar interaction pattern for both enantiomers, in that the sulfur atom contacts the zinc ion and the charged His158 residue in both cases. Conversely, the phenyl isoxazole moiety of the *R* isomer is able to stabilize hydrophilic interactions between two arginine residues (Arg37 and Arg154) that characterize the cavity rim of HDAC4. This finding is in agreement with the weak monodentate chelation observed with the clas-

 © 2012 Wiley-VCH Verlag GmbH & Co. KGaA, Weinheim

s IIa isoforms due to the lack of a conserved tyrosine residue, which globally renders the obtained complexes less dependent on interactions with the metal ion and more dependent on interactions with the cap group and linker.

As depicted in Figure 1b, the binding modes observed between the two enantiomers, (*R*)-**7b** and (*S*)-**7b**, and HDAC6 are similar to what was observed with HDAC2. The sulfur atom of the ZBG of both enantiomers contacts the zinc ion and protonated His610; however, only the carbonyl group of the *R* isomer's ZBG is able to interact with the zinc ion, allowing bidentate chelation. In addition, the sulfur atom of the *R* isomer's ZBG also contacts Tyr782. These putative complexes suggest the importance of bidentate chelation to the zinc ion with regard to activity, and also suggest the plausible role of Tyr782 in further stabilizing the thiol group. The various interactions stabilized by the cap group moieties also seem to possess a relevant role in HDAC6 binding, as the phenyl isoxazole group of the *R* isomer elicits hydrogen bonding interactions with Asp567 and Ser568, while the cap group of the *S* isomer assumes a more lateral arrangement, stabilizing only weak hydrophobic contacts.

Altogether, the docking results confirm the differences in selectivity observed between the considered subtypes which, based on these calculations, result from the different roles of the ZBG and cap group moieties in determining the binding mode. Interestingly, the different binding modes observed between the ZBG of each enantiomer and HDAC2 are essentially due to the different residues surrounding the metal ion; however, they may also be due to the presence of the adjacent foot cavity, which characterizes the binding pocket of the class I subtypes and allows for greater diversity amongst the computed poses, which is reflected by a greater difference in computed energy scores.

Finally, it was interesting to observe how the various arrangements of the linker, despite its flexibility, have a constraining effect on the interactions stabilized by the cap group (especially with regard to the class II isozymes). This is probably a result of the rigidity induced by the two amido functionalities.

Mercaptoacetamide dimerization

To determine if the addition of α-methyl groups relative to the thiol in these mercaptoacetamides increases resistance to dimerization, three ligands, **7a**, (*R*)-**7b**, and **7c**, were assayed by LC–MS to determine their qualitative rate of dimerization (Figure 2). We found that compound **7a**, which contains no methyl groups, dimerized at a much greater rate than both the monomethyl, (*R*)-**7b**, and dimethyl, **7c**, compounds. In comparing compounds (*R*)-**7b** and **7c**, we found that the addition of a second methyl group adjacent to the thiol further decreases the rate of dimerization; however, this decrease was not nearly as significant as the addition of the first methyl group.

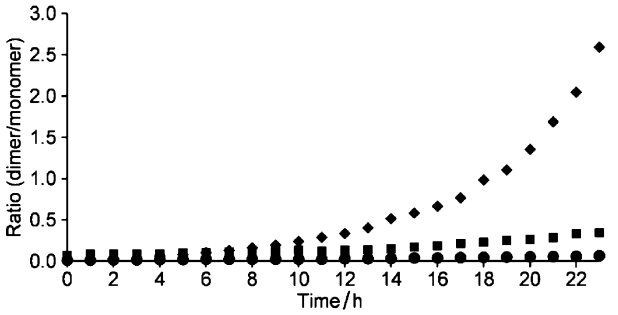

Figure 2. Qualitative determination of the rate of dimerization for compounds **7a** (◆), (*R*)-**7b** (■), and **7c** (●) as measured by LC–MS.

Neuroprotection and glutathione depletion

Treating central nervous system diseases with HDAC inhibitors, especially HDAC6 inhibitors, is viewed as a rational therapeutic approach. Therefore, our ligands were tested for their ability to provide primary cortical neuron protection in an in vitro model of oxidative stress-induced neurodegeneration.[30,31] In this model, neurodegeneration is induced by the presence of the cysteine homologue, homocysteine, at 5 mM, which depletes the cellular antioxidant glutathione via competitive inhibition of cysteine uptake at the plasma membrane cysteine/glutamate antiporter. Because cysteine is required for the synthesis of glutathione, the inhibition of its uptake results in glutathione depletion. Cellular redox homeostasis therefore becomes disrupted which leads to accumulation of endogenously produced and unopposed oxidants, resulting in neuronal degeneration over the course of approximately 24 hours. Importantly, primary neurons at this early developmental stage lack ionotropic and metabotropic receptors and are not susceptible to excitotoxicity; rather, cell death is induced by the accumulation of unopposed free radicals, and the neurons exhibit a number of apoptotic features.

At 10 μM, the hydroxamic acid **9** shows little neuroprotective activity, but does exhibit some toxicity, which was not observed with the mercaptoacetamides. Compound **7a**, which displays good HDAC6 activity, is moderately neuroprotective at 7.5 μM and fully neuroprotective at 10 μM, while the prodrug **6d** is moderately neuroprotective at 5 μM and fully neuroprotective at 7.5 μM (Figure 3a, 3b, and Supporting Information figure 5). It has been established that thioesters help to improve cell permeability by acting as prodrugs for the active thiols, which are released once they enter the cell.[24,27,32,33] Therefore, it is likely that **6d** is metabolized to **7a** inside the cell and that **7a** is responsible for the observed neuroprotective properties. Furthermore, the thioester prodrug **6d** may exhibit greater cell permeability than the mercaptoacetamide **7a** which would explain the lower concentrations of **6d** required to exhibit neuroprotection.[34] The same trend was also observed for the geometric isomers of **13a**, *cis*-**13a** and *trans*-**13a**, and their respective prodrugs, *cis*-**13d** and *trans*-**13d**. Alkene-linked mercaptoacetamides *cis*-**13a** and *trans*-**13a** display moderate neuroprotective activity at 20 μM and full neuroprotection at 50–100 μM, whereas their respective prodrugs,

 © 2012 Wiley-VCH Verlag GmbH & Co. KGaA, Weinheim

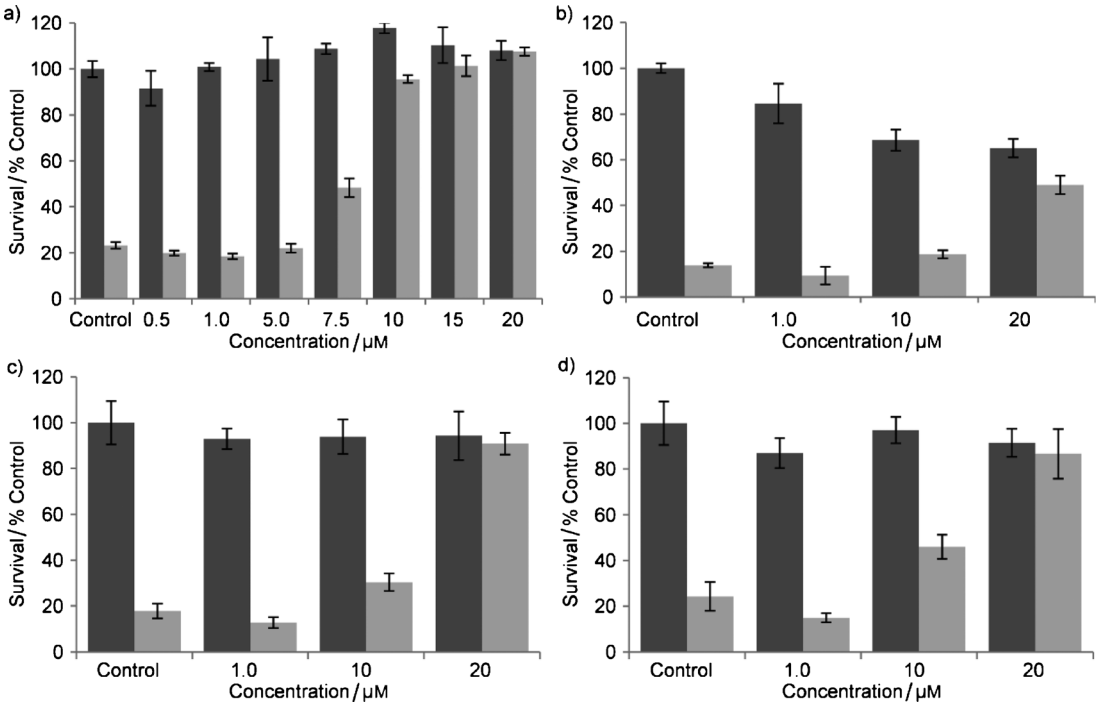

Figure 3. Neuroprotection plots for compounds a) **7a**, b) **9**, c) (*R*)-**7b**, and d) (*S*)-**7b**. Rat primary cortical neurons were incubated with varying concentrations of each compound either with (■) or without (■) 5 mM HCA for 24 h, after which cell viability was determined using an MTT assay.

cis-**13d** and *trans*-**13d**, are neuroprotective at 10 μM, but devoid of any significant HDAC activity (Supporting Information figure 5).

The monomethyl mercaptoacetamides **13b**, **18a**, and **18b** displayed neuroprotective activities that correlate well with their HDAC6 inhibitory activity. Compounds **18a** and **18b** displayed IC_{50} values at HDAC6 between 1 and 3 μM and are neuroprotective at 10 μM in vitro. Compound **13b**, however, is 3–12-fold less potent then the other monomethyl mercaptoacetamides in the enzyme assay. This was reflected by the need to use concentrations of 20 μM to effect neuroprotection. Compound **7c** did not display any neuroprotective activity which is consistent with the results of the HDAC6 enzyme inhibition assay (Supporting Information figure 5).

For some compounds, however, the activity at HDAC6 failed to track closely with the observed neuroprotective activity. Compounds (*R*)-**7b** and (*S*)-**7b** displayed peculiar neuroprotective profiles such that while compound (*R*)-**7b** is neuroprotective as expected, compound (*S*)-**7b** is also neuroprotective, although it does not display HDAC6 activity (Figure 3c and 3d). The same trend was observed with (*R*)-**16** and (*S*)-**16**. Compounds **13c**, **18c**, **18d**, **18e**, **20a**, and **20b** are also neuroprotective but show no activity at HDAC6, suggesting that an off-target mechanism may play a role in the neuroprotective properties of these compounds (Supporting Information figure 5).

Therefore, the ability of selected compounds to prevent glutathione depletion was measured (Figure 4). We found that (*S*)-**7b**, but not (*R*)-**7b**, is able to prevent glutathione depletion, suggesting this as an additional neuroprotective pathway for these compounds. Moreover, **7a** is also very effective in preventing glutathione depletion which likely contributes to the excellent neuroprotective profile observed with this compound. A similar albeit less pronounced effect was observed with (*R*)-**16** and (*S*)-**16**, in that the *S* isomer is more effective in preventing glutathione depletion than the *R* isomer. Many of the other compounds tested displayed a moderate ability to prevent glutathione depletion, including *cis*- and *trans*-**13a** as well as their respective prodrugs, *cis*- and *trans*-**13d**.

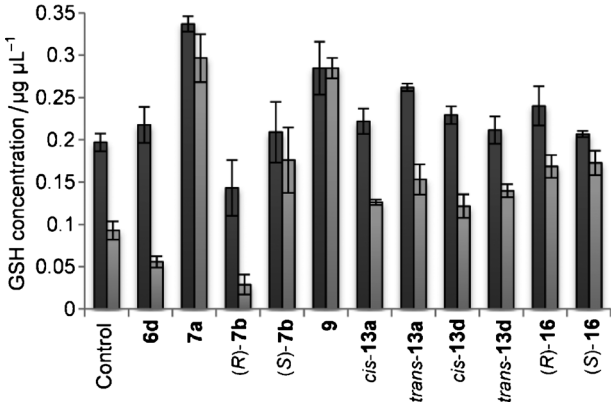

Figure 4. Prevention of glutathione depletion by selected mercaptoacetamides. Rat primary cortical neurons were incubated with each compound at 10 μM in the absence (■) or presence (■) of the cysteine homologue HCA (5 mM).

Of note, however, is compound **9**, which is able to prevent glutathione depletion without being neuroprotective. This is likely due to the intrinsic neuronal toxicity that is often observed with hydroxamic acids: although this compound is active at HDAC6 and is able to prevent glutathione depletion,

 © 2012 Wiley-VCH Verlag GmbH & Co. KGaA, Weinheim

the aforementioned ZBG precludes any substantial neuroprotective activity. When dealing with epigenetic regulators (and small molecules in general), it is unlikely that only one biological pathway will be affected and thus the neuroprotective activity of these compounds probably results from a combination of effects. In addition to HDAC6 inhibition and the prevention of glutathione depletion, other mechanisms that may contribute to the observed neuroprotective activity of these compounds include the inhibition of MMPs and other zinc-dependent enzymes, interference with HCA itself, and/or the intrinsic antioxidant activity of the thiols themselves.[35] Therefore, further investigation into the potential neuroprotective mechanisms of these compounds is necessary to fully elucidate all of the biological pathways involved.

Conclusions

Two HDACIs are currently marketed for the treatment of cutaneous T-cell lymphoma, and a host of others are the subjects of ongoing clinical trials.[36] The continued development of novel HDACIs as therapeutics is warranted; however, the majority of the reported compounds lack isozyme selectivity, thus leading to various levels of undesirable toxicity. While pan-activity may be acceptable for oncology applications, it is unlikely to be acceptable in other therapeutic areas. As detailed herein, we have developed a series of selective, stable, low-molecular-weight HDAC6 inhibitors that exhibit neuroprotection in neuronal models of oxidative stress for potential use in the treatment of neurodegenerative diseases, traumatic brain injury, and other health problems, such as myocardial infarction, in which oxidative stress is an issue. We demonstrated that mercaptoacetamide **7a** (HDAC1 $IC_{50}=5.7\ \mu M$, HDAC6 $IC_{50}=0.26\ \mu M$) exhibits potency and selectivity similar to that of the hydroxamic acid analogue **9** (HDAC1 $IC_{50}=3.0\ \mu M$, HDAC6 $IC_{50}=0.18\ \mu M$). Therefore, mercaptoacetamide ZBGs may find potential use in place of the traditional hydroxamic acids. In addition, replacement of the hydroxamic acid functionality with a mercaptoacetamide alleviates the toxicity observed in cortical neurons, suggesting this as a suitable approach toward an improved safety profile. Selective inhibition of HDAC6 also results in dose-dependent protection against oxidative stress in cultured cortical neurons, further supporting the idea that HDAC6 inhibition may be a viable way to treat certain neurological diseases.[30] Therefore, HDAC6-selective mercaptoacetamides offer an attractive alternative to the conventional hydroxamic acid based inhibitors, as they afford a decrease in toxicity and the potential for enhanced cell permeability via prodrug formation.

Experimental Section

Chemistry

^1H NMR and ^{13}C NMR spectra were recorded on a Bruker spectrometer at 300/400 MHz and 75/100 MHz, respectively, with TMS as an internal standard. Standard abbreviations indicating multiplicity were used: s = singlet, d = doublet, t = triplet, q = quartet, m = multiplet, dd = doublet of doublets, dt = doublet of triplets, and br = broad. HRMS experiments were performed on a Q-TOF-2TM instrument (Micromass). TLC was performed with Merck 250 mm 60 F_{254} silica gel plates. Column chromatography was performed with Merck silica gel (40–60 mesh). Microwave-assisted reactions were carried out in a sealed tube using a Biotage Initiator. Preparative HPLC was carried out with an ACE 5AQ column (250×10 mm) on a Shimadzu LC8A with SPD-10avp detector (λ 254 and 280 nm) and a flow rate of 3.5 mL min^{-1} with a gradient (Method A: from 30% CH_3CN in H_2O to 100% CH_3CN over 30 min; Method B: from 10% CH_3CN in H_2O to 100% CH_3CN over 28 min). Chiral HPLC was carried out with a Chiralpak AD column (250×10 mm) on a Shimadzu LC8A with SPD-10AV detector (λ 230 and 240 nm) and a flow rate of 2.4 mL min^{-1} with an isocratic mobile phase (80:20 hexane/2-propanal). The purity of all tested compounds was $\geq$95%, as determined by analytical HPLC (Agilent 1100 with a G1314A detector (λ 254 nm) and a flow rate of 1.4 mL min^{-1} using a Synergi 4 μ hydro-RP column (150×4.6 mm) or a Luna 5 μ C_{18} column (150×4.6 mm) and a gradient from 60% CH_3CN in H_2O to 100% CH_3CN over 25 min).

Ethyl 5-methyl-3-phenylisoxazole-4-carboxylate (1): (*E*)-benzaldehyde oxime (2.4 g, 19.8 mmol) was mixed with neutral Al_2O_3 (20 g). *N*-chlorosuccinimide (3.0 g, 22.4 mmol) was added, and the reaction mixture was irradiated at 40 °C for 3×10 min, mixing between each step. The mixture was extracted with CCl_4 (40 mL), and the solvent was evaporated. The obtained yellow oil was dissolved in anhydrous THF (30 mL). Ethyl 2-butynoate (1.16 mL, 10.0 mmol) and Et_3N (6.0 mL, 43.0 mmol) were added slowly. The reaction mixture was irradiated at 70 °C for 1 h, filtered and washed with EtOAc, and then the filtrate was concentrated in vacuo. Purification of the crude reaction mixture by column chromatography (SiO_2, 0→10% EtOAc/hexanes) afforded the title compound (1.0 g, 43%) as a pale-yellow oil. ^1H NMR (400 MHz, $CDCl_3$): $\delta=7.62$–7.60 (m, 2H), 7.43–7.38 (m, 3H), 4.21 (q, $J=7.2$ Hz, 2H), 2.70 (s, 3H), 1.92 ppm (t, $J=7.2$ Hz, 3H); ^{13}C NMR (100 MHz, $CDCl_3$): $\delta=175.6$, 162.3, 161.7, 129.6, 129.2, 128.5, 127.9, 108.2, 60.5, 13.7, 13.3 ppm.

5-Methyl-3-phenylisoxazole-4-carboxylic acid (2): NaOH (540 mg, 13.3 mmol) was added to isoxazole **1** (2.68 g, 11.6 mmol) in CH_3OH/H_2O 1:1 (80 mL). The reaction mixture was stirred at 60 °C for 4 h, and then the CH_3OH layer was evaporated. The aqueous layer was acidified with 1 N HCl to pH 3 and then extracted with EtOAc (3×50 mL). The combined organic layers were washed with H_2O (100 mL), brine (50 mL), and dried over anhydrous Na_2SO_4 to afford the title compound (2.31 g, 98%) as a white powder. ^1H NMR (400 MHz, $CDCl_3$): $\delta=7.65$–7.62 (m, 2H), 7.49–7.43 (m, 3H), 2.77 ppm (s, 3H); ^{13}C NMR (100 MHz, $CDCl_3$): $\delta=177.7$, 166.8, 162.7, 129.9, 129.4, 128.2, 127.9, 107.5, 13.9 ppm.

***tert*-Butyl 5-(5-methyl-3-phenylisoxazole-4-carbonylamino)pentylcarbamate (3)**: *N*-Boc-1,5-diaminopentane (2.6 mL, 12.6 mmol), PyBOP (7.12 g, 13.7 mmol), and diisopropylethylamine (DIEA, 6 mL, 34.2 mmol) were added to isoxazole **2** (2.32 g, 11.4 mmol) in CH_2Cl_2 (100 mL). The reaction mixture was stirred at room temperature for 20 h and quenched with H_2O. The aqueous layer was extracted with CH_2Cl_2 (3×50 mL). The combined organic layers were washed with brine (50 mL) and dried over anhydrous Na_2SO_4. Purification of the crude reaction mixture by column chromatography (SiO_2, 0→20% EtOAc/hexanes) afforded the title compound (4.35 g, 98%) as a white powder. ^1H NMR (400 MHz, $CDCl_3$): $\delta=7.49$–7.47 (m, 2H), 7.39–7.36 (m, 3H), 5.82 (br, 1H), 4.71 (br, 1H), 3.13–3.08 (m, 2H), 2.94–2.89 (m, 2H), 2.54 (s, 3H), 1.32 (s, 9H), 1.28–1.22 (m, 4H), 1.08–1.03 ppm (m, 2H); ^{13}C NMR (100 MHz, $CDCl_3$): $\delta=172.4$, 161.2, 159.6, 155.6, 129.9, 128.5, 128.3, 127.8, 111.1, 78.5, 38.8, 29.1, 28.3, 27.9, 25.9, 25.8, 12.2 ppm.

 © 2012 Wiley-VCH Verlag GmbH & Co. KGaA, Weinheim

Methyl-3-phenylisoxazole-4-carboxylic acid (5-aminopentyl)amide TFA (4): Trifluoroacetic acid (TFA, 7.7 mL, 103.7 mmol) was added to isoxazole **3** (4.02 g, 10.4 mmol) in CH_2Cl_2 (60 mL). The reaction mixture was stirred at room temperature for 4 h, and then the solvent was removed in vacuo to afford the title compound (4.09 g, 98%) as a yellow oil. ^{1}H NMR (400 MHz, CD_3OD): δ = 7.61–7.57 (m, 2H), 7.43–7.39 (m, 3H), 3.27–3.23 (m, 2H), 2.84–2.80 (m, 2H), 2.49 (s, 3H), 1.68–1.58 (m, 2H), 1.54–1.47 (m, 2H), 1.34–1.26 ppm (m, 2H); ^{13}C NMR (100 MHz, CD_3OD): δ = 171.6, 164.6, 161.9, 131.2, 129.8, 129.2, 128.1, 113.8, 40.5, 40.3, 29.6, 28.0, 24.7, 12.0 ppm.

Tritylsulfanylacetic acid (5a): CPh_3OH (13.0 g, 50 mmol) and TFA (5.0 mL, 65 mmol) were added to thioglycolic acid (3.5 mL, 50 mmol) in $CHCl_3$ (50 mL). The reaction mixture was stirred at room temperature for 3 h. The volatiles were removed in vacuo. The crude product was recrystallized from CH_2Cl_2/hexanes 1:1 (30 mL) and washed with cold Et_2O to afford the title compound (15.9 g, 95%) as a white powder. ^{1}H NMR (300 MHz, $CDCl_3$): δ = 7.43–7.40 (m, 6H), 7.30–7.19 (m, 9H), 3.02 ppm (s, 2H); ^{13}C NMR (75 MHz, CD_3OD): δ = 171.7, 144.2, 129.3, 127.6, 126.6, 66.7, 34.3 ppm.

2-Tritylsulfanylpropionic acid (5b): Compound **5b** (75%) was prepared from 2-mercaptopropanoic acid according to the methodology described for **5a**. ^{1}H NMR (400 MHz, CD_3OD): δ = 7.43–7.41 (m, 6H), 7.28–7.19 (m, 9H), 2.90 (q, J = 7.2 Hz, 1H), 1.01 ppm (d, J = 7.2 Hz, 3H); ^{13}C NMR (100 MHz, CD_3OD): δ = 177.1, 145.8, 130.8, 128.9, 127.9, 69.3, 44.0, 19.4 ppm.

2-Tritylsulfanylisobutyric acid (5c): Compound **5c** (80%) was prepared from 2-mercaptoisobutyric acid according to the methodology described for **5a**. ^{1}H NMR (400 MHz, $CDCl_3$): δ = 7.68–7.66 (m, 6H), 7.38–7.26 (m, 9H), 1.48 ppm (s, 6H); ^{13}C NMR (100 MHz, $CDCl_3$): δ = 180.0, 144.2, 129.9, 127.6, 126.7, 68.4, 51.2, 27.1 ppm.

Pivaloylsulfanylacetic acid (5d): Pivaloyl chloride (2.7 mL, 22 mmol) and Et_3N (6.1 mL, 44 mmol) were added to thioglycolic acid (1.39 mL, 50 mmol) in dioxane (10 mL) at 0 °C. The reaction mixture was stirred at room temperature overnight, filtered and acidified with 1 N HCl to pH 1. This layer was extracted with CH_2Cl_2 (3×100 mL). The combined organic layers were dried over anhydrous Na_2SO_4. Purification of the crude reaction mixture by preparative HPLC Method B afforded the title compound (0.61 g, 17%) as a colorless oil. ^{1}H NMR (300 MHz, $CDCl_3$): δ = 9.80 (s, 1H), 3.52 (s, 2H), 1.89 ppm (s, 9H); ^{13}C NMR (75 MHz, CD_3OD): δ = 205.1, 174.7, 46.2, 30.8, 27.0 ppm.

5-Methyl-3-phenylisoxazole-4-carboxylic acid [5-(2-tritylsulfanylacetyl)aminopentyl]amide (6a): Compound **5a** (3.85 g, 11.5 mmol), PyBOP (7.0 g, 13.4 mmol), and DIEA (5 mL, 29.0 mmol) were added to isoxazole **4** (3.85 g, 9.6 mmol) in CH_2Cl_2 (100 mL). The reaction mixture was stirred at room temperature for 20 h and quenched with H_2O. The aqueous layer was extracted with CH_2Cl_2 (3×50 mL). The combined organic layers were washed with brine (50 mL) and dried over anhydrous Na_2SO_4. Purification of the crude reaction mixture by column chromatography (SiO_2, 0→5% CH_3OH/CH_2Cl_2) afforded the title compound (5.32 g, 92%) as a white foam. ^{1}H NMR (400 MHz, $CDCl_3$): δ = 7.58–7.55 (m, 2H), 7.53–7.49 (m, 3H), 7.42–7.38 (m, 6H), 7.31–7.20 (m, 9H), 5.97 (br, 1H), 5.38 (br, 1H), 3.21–3.17 (m, 2H), 3.09 (s, 2H), 2.89–2.85 (m, 2H), 2.71 (s, 3H), 1.32–1.23 (m, 4H), 1.05–1.01 ppm (m, 2H); ^{13}C NMR (100 MHz, $CDCl_3$): δ = 173.3, 167.7, 161.4, 159.9, 143.8, 130.3, 129.3, 128.9, 128.7, 128.1, 128.0, 126.9, 111.2, 67.7, 39.2, 38.9, 35.7, 28.6, 28.5, 23.8, 12.6 ppm.

5-Methyl-3-phenylisoxazole-4-carboxylic acid [5-(2-tritylsulfanylpropionyl)aminopentyl]amide (6b): Compound **6b** (73%) was prepared from compound **5b** according to the methodology described for **6a**. ^{1}H NMR (400 MHz, $CDCl_3$): δ = 7.59–7.56 (m, 2H), 7.51–7.47 (m, 3H), 7.44–7.42 (m, 6H), 7.30–7.22 (m, 6H), 7.21–7.19 (m, 3H), 6.01 (br, 1H), 5.75 (br, 1H), 3.21–3.16 (m, 2H), 3.02 (q, J = 7.6 Hz, 1H), 2.91–2.86 (m, 1H), 2.67–2.62 (m, 1H), 2.66 (s, 3H), 1.43 (d, J = 7.6 Hz, 2H), 1.33–1.28 (m, 2H), 1.24–1.20 (m, 2H), 1.08–1.02 ppm (m, 2H); ^{13}C NMR (100 MHz, $CDCl_3$): δ = 173.0, 172.4, 161.5, 159.9, 144.1, 130.3, 129.1, 128.8, 128.6, 128.0, 127.9, 126.8, 111.2, 67.9, 44.3, 39.2, 39.0, 28.5, 28.4, 23.7, 19.9, 12.6 ppm.

(*R*)-5-Methyl-3-phenylisoxazole-4-carboxylic acid [5-(2-tritylsulfanylpropionyl)aminopentyl]amide ((*R*)-6b): Compound (*R*)-**6b** was isolated from the racemic mixture of compound **6b** using chiral preparative HPLC as described in the synthetic protocol above. ^{1}H NMR (400 MHz, $CDCl_3$): δ = 7.59–7.56 (m, 2H), 7.51–7.48 (m, 3H), 7.44–7.42 (m, 6H), 7.31–7.27 (m, 6H), 7.24–7.20 (m, 3H), 5.92 (br, 1H), 5.46 (br, 1H), 3.22–3.17 (m, 2H), 3.02 (q, J = 7.6 Hz, 1H), 2.92–2.87 (m, 1H), 2.71 (s, 3H), 2.69–2.61 (m, 1H), 1.43 (d, J = 7.6 Hz, 3H), 1.33–1.27 (m, 2H), 1.25–1.20 (m, 2H), 1.07–1.02 ppm (m, 2H); ^{13}C NMR (100 MHz, $CDCl_3$): δ = 174.0, 172.4, 161.6, 160.2, 144.5, 130.7, 129.5, 129.3, 129.1, 128.5, 128.3, 127.2, 110.9, 68.3, 44.7, 39.6, 39.3, 28.9, 28.8, 24.1, 20.4, 13.1 ppm; $[\alpha]_D^{20} = +39.9$ (c = 1, $CHCl_3$).

(*S*)-5-Methyl-3-phenylisoxazole-4-carboxylic acid [5-(2-tritylsulfanylpropionyl)aminopentyl]amide ((*S*)-6b): Compound (*S*)-**6b** was isolated from the racemic mixture of compound **6b** using chiral preparative HPLC as described in the synthetic protocol above. ^{1}H NMR (400 MHz, $CDCl_3$): δ = 7.58–7.56 (m, 2H), 7.53–7.49 (m, 3H), 7.43–7.41 (m, 6H), 7.30–7.28 (m, 6H), 7.26–7.19 (m, 3H), 5.93 (br, 1H), 5.44 (br, 1H), 3.20–3.18 (m, 2H), 3.02 (q, J = 7.6 Hz, 1H), 2.93–2.86 (m, 1H), 2.70 (s, 3H), 2.68–2.62 (m, 1H), 1.43 (d, J = 7.6 Hz, 3H), 1.32–1.28 (m, 2H), 1.23–1.19 (m, 2H), 1.04–1.02 ppm (m, 2H); ^{13}C NMR (100 MHz, $CDCl_3$): δ = 173.5, 172.1, 161.2, 159.6, 143.9, 130.1, 129.0, 128.7, 128.6, 127.9, 127.7, 126.6, 110.7, 67.8, 44.1, 39.1, 38.7, 28.3, 28.2, 23.6, 19.8, 12.5 ppm; $[\alpha]_D^{20} = -36.5$ (c = 1, $CHCl_3$).

5-Methyl-3-phenylisoxazole-4-carboxylic acid [5-(2-tritylsulfanylisobutyryl)aminopentyl]amide (6c): Compound **6c** (98%) was prepared from compound **5c** according to the methodology described for **6a**. ^{1}H NMR (400 MHz, $CDCl_3$): δ = 7.59–7.56 (m, 2H), 7.47–7.45 (m, 3H), 7.44–7.42 (m, 6H), 7.26–7.22 (m, 6H), 7.20–7.17 (m, 3H), 6.49 (br, 1H), 6.01 (br, 1H), 3.20–3.15 (m, 2H), 3.10–3.05 (m, 2H), 2.62 (s, 3H), 1.35 (s, 6H), 1.33–1.28 (m, 2H), 1.19–1.13 (m, 2H), 1.07–1.02 ppm (m, 2H); ^{13}C NMR (100 MHz, $CDCl_3$): δ = 174.1, 172.5, 161.9, 160.2, 144.4, 130.3, 129.1, 129.0, 128.6, 128.0, 127.8, 126.9, 111.7, 67.9, 52.3, 43.3, 39.3, 28.6, 28.5, 28.4, 23.9, 12.6 ppm.

5-Methyl-3-phenylisoxazole-4-carboxylic acid [5-(2-pivaloylsulfanylacetyl)aminopentyl]amide (6d): Compound **6d** (14%) was prepared from compound **5d** according to the methodology described for **6a**. Purification of the obtained crude mixture was done using preparative HPLC Method A. ^{1}H NMR (400 MHz, $CDCl_3$): δ = 7.59–7.57 (m, 2H), 7.54–7.49 (m, 3H), 6.22 (br, 1H), 5.46 (br, 1H), 3.45 (s, 2H), 3.24–3.19 (m, 2H), 3.17–3.12 (m, 2H), 2.71 (s, 3H), 1.42–1.31 (m, 4H), 1.24 (s, 9H), 1.16–1.11 ppm (m, 2H); ^{13}C NMR (100 MHz, $CDCl_3$): δ = 207.26, 173.8, 168.7, 161.6, 160.0, 130.5, 129.1, 129.0, 128.3, 111.1, 46.5, 39.3, 39.1, 32.4, 28.9, 28.7, 27.2, 23.7, 12.9 ppm; ESI-HRMS calcd for $[C_{23}H_{31}N_3O_4S+H]^+$: 426.21080 m/z, found: 426.2130 m/z; HPLC purity: 98.0%.

5-Methyl-3-phenylisoxazole-4-carboxylic acid [5-(2-mercaptoacetyl)aminopentyl]amide (7a): TFA (6.5 mL, 88.0 mmol) and triethylsilane (2.8 mL, 17.6 mmol) were added to isoxazole **6a** (5.31 g, 8.8 mmol) in CH_2Cl_2 (50 mL) at 0 °C. The reaction mixture was

 © 2012 Wiley-VCH Verlag GmbH & Co. KGaA, Weinheim

stirred at room temperature for 3 h. DMF (2 mL) was added, and volatiles were removed in vacuo. Purification of the crude reaction mixture by preparative HPLC Method A afforded the title compound (2.45 g, 77%) as a white powder. ^{1}H NMR (400 MHz, $CDCl_3$): δ = 7.59–7.54 (m, 2H), 7.52–7.48 (m, 3H), 6.70 (br, 1H), 5.44 (br, 1H), 3.26–3.20 (m, 6H), 2.71 (s, 3H), 1.85 (t, J = 9.0 Hz, 1H), 1.51–1.44 (m, 2H), 1.41–1.34 (m, 2H), 1.22–1.14 ppm (m, 2H); ^{13}C NMR (100 MHz, $CDCl_3$): δ = 173.7, 169.1, 161.5, 160.0, 130.5, 129.1, 128.9, 128.2, 111.1, 39.5, 39.0, 28.9, 28.7, 28.2, 23.8, 12.8 ppm; ESI-HRMS calcd for $[C_{18}H_{23}N_3O_3S+H]^+$: 362.15329 *m/z*, found: 362.1519 *m/z*; HPLC purity: 99.7%.

5-Methyl-3-phenylisoxazole-4-carboxylic acid [5-(2-mercaptopropionyl)aminopentyl]amide (7b): Compound **7b** (46%) was prepared from compound **6b** according to the methodology described for **7a**. ^{1}H NMR (400 MHz, $CDCl_3$): δ = 7.57–7.55 (m, 2H), 7.54–7.47 (m, 3H), 6.54 (br, 1H), 5.50 (br, 1H), 3.40–3.35 (m, 1H), 3.24–3.15 (m, 4H), 2.69 (s, 3H), 1.99 (d, J = 8.4 Hz, 1H), 1.50 (d, J = 7.2 Hz, 3H), 1.47–1.42 (m, 2H), 1.40–1.34 (m, 2H), 1.21–1.15 ppm (m, 2H); ^{13}C NMR (100 MHz, $CDCl_3$): δ = 173.7, 172.8, 161.5, 160.0, 130.5, 129.1, 128.9, 128.2, 111.1, 39.4, 39.0, 38.1, 28.8, 28.7, 23.8, 22.2, 12.8 ppm; ESI-HRMS calcd for $[C_{19}H_{25}N_3O_3S+H]^+$: 376.16894 *m/z*, found: 376.1692 *m/z*; HPLC purity: 98.9%.

(*R*)-5-Methyl-3-phenylisoxazole-4-carboxylic acid [5-(2-mercaptopropionyl)aminopentyl]amide ((*R*)-7b): Compound (*R*)-**7b** (43%) was prepared from compound (*R*)-**6b** according to the methodology described for **7a**. ^{1}H NMR (400 MHz, $CDCl_3$): δ = 7.57–7.54 (m, 2H), 7.54–7.50 (m, 3H), 6.56 (br, 1H), 5.53 (br, 1H), 3.40–3.36 (m, 1H), 3.24–3.15 (m, 4H), 2.69 (s, 3H), 1.99 (d, J = 8.4 Hz, 1H), 1.50 (d, J = 7.2 Hz, 3H), 1.48–1.42 (m, 2H), 1.40–1.35 (m, 2H), 1.21–1.15 ppm (m, 2H); ^{13}C NMR (100 MHz, $CDCl_3$): δ = 173.3, 172.6, 161.2, 159.7, 130.1, 128.7, 128.5, 127.8, 110.8, 39.1, 38.6, 37.8, 28.5, 28.4, 23.5, 21.9, 12.5 ppm; $[\alpha]_D^{20}$ = +3.9 (c = 0.1, $CHCl_3$); ESI-HRMS calcd for $[C_{19}H_{25}N_3O_3S+H]^+$: 376.1689 *m/z*, found: 376.1692 *m/z*; HPLC purity: 98.7%.

(*S*)-5-Methyl-3-phenylisoxazole-4-carboxylic acid [5-(2-mercaptopropionyl)aminopentyl]amide ((*S*)-7b): Compound (*S*)-**7b** (45%) was prepared from compound (*S*)-**6b** according to the methodology described for **7a**. ^{1}H NMR (400 MHz, $CDCl_3$): δ = 7.58–7.55 (m, 2H), 7.53–7.48 (m, 3H), 6.51 (br, 1H), 5.48 (br, 1H), 3.41–3.37 (m, 1H), 3.25–3.16 (m, 4H), 2.70 (s, 3H), 1.99 (d, J = 8.4 Hz, 1H), 1.50 (d, J = 7.2 Hz, 3H), 1.46–1.43 (m, 2H), 1.38–1.33 (m, 2H), 1.21–1.15 ppm (m, 2H); ^{13}C NMR (100 MHz, $CDCl_3$): δ = 174.0, 173.1, 161.8, 160.2, 130.7, 129.3, 129.2, 128.5, 111.4, 39.7, 39.2, 38.4, 29.1, 29.0, 24.1, 22.5, 13.1 ppm; $[\alpha]_D^{20}$ = −3.7 (c = 0.1, $CHCl_3$); ESI-HRMS calcd for $[C_{19}H_{25}N_3O_3S+H]^+$: 376.1689 *m/z*, found: 376.1691 *m/z*; HPLC purity: 99.0%.

5-Methyl-3-phenylisoxazole-4-carboxylic acid [5-(2-mercaptoisobutyryl)aminopentyl]amide (7c): Compound **7c** (57%) was prepared from compound **6c** according to the methodology described for **7a**. ^{1}H NMR (400 MHz, $CDCl_3$): δ = 7.54–7.50 (m, 2H), 7.47–7.43 (m, 3H), 6.96 (br, 1H), 5.63 (br, 1H), 3.21–3.16 (m, 2H), 3.15–3.10 (m, 2H), 2.64 (s, 3H), 2.14 (s, 1H), 1.52 (S, 6H), 1.46–1.38 (m, 2H), 1.36–1.30 (m, 2H), 1.17–1.09 ppm (m, 2H); ^{13}C NMR (100 MHz, $CDCl_3$): δ = 175.1, 173.3, 161.5, 159.9, 130.3, 129.0, 128.7, 128.1, 111.1, 47.5, 39.6, 39.0, 30.2, 28.9, 28.6, 23.8, 12.7 ppm; ESI-HRMS calcd for $[C_{20}H_{27}N_3O_3S+H]^+$: 390.1846 *m/z*, found: 390.1861 *m/z*; HPLC purity: 99.0%.

Methyl 7-(5-methyl-3-phenylisoxazole-4-carbonylamino)heptanoate (8): Methyl 5-aminopentanoate (generated from its acid, 0.193 g, 1.0 mmol), benzotriazol-1-yl-oxytripyrrolidinophosphonium hexafluorophosphate (PyBOP, 0.612 g, 1.2 mmol), and DIEA (0.5 mL, 3 mmol) were added to isoxazole **2** (0.2 g, 1.0 mmol) in CH_2Cl_2 (20 mL). The reaction mixture was stirred at room temperature for 20 h and then quenched with H_2O. The aqueous layer was extracted with CH_2Cl_2 (3×30 mL). The combined organic layers were washed with brine (30 mL) and dried over anhydrous Na_2SO_4. Purification of the crude reaction mixture by column chromatography (SiO_2, 0→5% CH_3OH/CH_2Cl_2) afforded the title compound (0.29 g, 86%) as a white solid. ^{1}H NMR (400 MHz, $CDCl_3$): δ = 7.43–7.41 (m, 2H), 7.36–7.27 (m, 3H), 5.91 (br, 1H), 3.49 (s, 3H), 3.07–3.02 (m, 2H), 2.46 (s, 3H), 2.13 (t, J = 7.2 Hz, 2H), 1.46–1.37 (m, 2H), 1.24–1.18 (m, 2H), 1.13–1.05 (m, 2H), 1.03–2.97 ppm (m, 2H); ^{13}C NMR (100 MHz, $CDCl_3$): δ = 173.6, 172.1, 161.2, 159.7, 129.9, 128.2, 127.8, 126.7, 111.3, 51.0, 38.9, 33.4, 28.5, 28.2, 26.0, 24.3, 12.1 ppm.

5-Methyl-3-phenylisoxazole-4-carboxylic acid (6-hydroxycarbamoylhexyl)amide (9): NH_2OH [generated from filtration at 0 °C of a mixture of $NH_2OH{\cdot}HCl$ (0.4 g, 5.8 mmol) and KOH (325 mg, 5.8 mmol) in CH_3OH (2 mL) heated at 40 °C] and KOH (120 mg, 2.1 mmol) were added to isoxazole **8** (0.1 g, 0.29 mmol) in CH_3OH (1 mL). The reaction mixture was stirred at room temperature for 1.5 h and quenched with H_2O. The aqueous layer was extracted with EtOAc (3×10 mL). The combined organic layers were dried over anhydrous Na_2SO_4. Purification of the crude reaction mixture by preparative HPLC Method A afforded the title compound (0.21 g, 21%) as a white solid. ^{1}H NMR (400 MHz, CD_3OD): δ = 8.20 (br, 1H), 7.66–7.64 (m, 2H), 7.52–7.44 (m, 3H), 3.31–3.27 (m, 2H), 2.54 (s, 3H), 2.08 (t, J = 7.2 Hz, 2H), 1.62–1.48 (m, 4H), 1.36–1.30 ppm (m, 4H); ^{13}C NMR (100 MHz, CD_3OD): δ = 171.5, 164.6, 161.9, 131.3, 129.8, 129.2, 129.1, 113.9, 40.6, 30.0, 29.7, 27.6, 26.6, 11.9 ppm; ESI-HRMS calcd for $[C_{18}H_{23}N_3O_4+H]^+$: 346.17613 *m/z*, found: 346.1768 *m/z*; HPLC purity: 96.2%.

5-Methyl-3-phenylisoxazol-4-ylmethanol (10): A borane–THF solution (1.5 mL, 1.0 M) was added dropwise to a solution of acid **2** (203 mg, 1 mmol) in anhydrous THF (10 mL) at 0 °C. The mixture was then stirred at room temperature overnight, after which the reaction was quenched with H_2O (10 mL), and the organic products were extracted with EtOAc (3×15 mL). The organic layer was washed with H_2O (10 mL), brine (10 mL) and dried over Na_2SO_4. After concentration in vacuo, the crude product was purified by column chromatography (SiO_2, EtOAc/hexanes 70:30→50:50) to afford the title product **10** (170 mg, 90%) as a colorless oil. ^{1}H NMR (400 MHz, $CDCl_3$): δ = 7.76–7.73 (m, 2H), 7.42–7.39 (m, 3H), 4.47 (s, 2H), 2.37 ppm (s, 3H); ^{13}C NMR (100 MHz, $CDCl_3$): δ = 168.5, 162.3, 129.6, 128.8, 128.7, 128.1, 112.9, 53.2, 10.9 ppm.

5-Methyl-3-phenylisoxazole-4-carbaldehyde (11): The alcohol **10** (190 mg, 1 mmol) and activated MnO_2 (870 mg, 10 mmol) were dissolved in anhydrous CH_2Cl_2 (5 mL) under Ar atmosphere. The mixture was stirred at room temperature overnight. After the black powder was filtered off, the filtrate was dried in vacuo and purified by column chromatography (SiO_2, EtOAc/hexanes 75:25) to afford the title product **11** (175 mg, 94%) as a white solid. ^{1}H NMR (400 MHz, $CDCl_3$): δ = 9.91 (s, 1H), 7.66–7.65 (m, 2H), 7.49–7.47 (m, 3H), 2.74 ppm (s, 3H); ^{13}C NMR (100 MHz, $CDCl_3$): δ = 184.3, 176.6, 162.0, 130.3, 128.8, 114.9, 12.8 ppm.

***tert*-Butyl 7-(5-methyl-3-phenylisoxazol-4-yl)hept-6-enylcarbamate (12)**: *n*-Butyllithium (10.8 mL, 17.3 mmol) was added to the *tert*-butyl 6-triphenyl-λ^5-phosphanylhexylcarbamate phosphonium salt (6.26 g, 11.5 mmol, generated from *tert*-butyl 6-bromohexylcarbamate and PPh_3 in toluene at reflux for four days) in THF (100 mL) at 0 °C. The reaction mixture was stirred at 0 °C for 30 min; then the aldehyde **11** (388 mg, 2.07 mmol) in THF (5 mL) was added. The reaction mixture was stirred at room temperature

 © 2012 Wiley-VCH Verlag GmbH & Co. KGaA, Weinheim

for 1.5 h and then quenched with H_2O (50 mL). The aqueous layer was extracted with EtOAc (3×60 mL). The combined organic layers were washed with brine (50 mL) and dried over anhydrous Na_2SO_4. Purification of the crude reaction mixture by column chromatography (SiO_2, 0→25% EtOAc/hexanes) afforded the title compound *Z*/*E* 8:2 (415 mg, 54%) as a yellow oil. ^{1}H NMR (400 MHz, $CDCl_3$): δ = 7.73–7.70 (m, 2H), 7.62–7.59 (m, 2H), 7.44–7.38 (m, 6H), 6.06–6.02 (m, 2H), 5.82–5.76 (m, 2H), 4.54 (br, 1H), 4.49 (br, 1H), 3.09–2.99 (m, 4H), 2.45 (s, 3H), 2.31 (s, 3H), 2.17–2.12 (m, 2H), 1.91–1.86 (m, 2H), 1.41 (s, 18H), 1.36–1.27 (m, 8H), 1.23–1.15 ppm (m, 4H); ^{13}C NMR (100 MHz, $CDCl_3$): δ = 166.0, 165.4, 161.0, 155.8, 136.7, 134.9, 129.7, 129.3, 128.4, 127.7, 117.6, 117.0, 112.5, 111.1, 78.9, 40.3, 33.2, 29.7, 28.8, 28.5, 28.3, 26.2, 12.0, 11.7 ppm.

***N*-[7-(5-Methyl-3-phenylisoxazol-4-yl)hept-6-enyl]-2-mercaptoacetamide (13a)**: Compound **13a** *Z*/*E* 7:3 (33%) was prepared from compound **12** in three steps according to the methodology described for **4**, **6a**, and **7a**. ^{1}H NMR (400 MHz, $CDCl_3$): δ = 7.75–7.72 (m, 2H), 7.63–7.61 (m, 2H), 7.45–7.41 (m, 6H), 6.97 (br, 1H), 6.60 (br, 1H), 6.09–6.05 (m, 2H), 5.84–5.74 (m, 2H), 3.28–3.15 (m, 4H), 2.47 (s, 3H), 2.33 (s, 3H), 1.94–1.89 (m, 2H), 1.84–1.80 (m, 2H), 1.56–1.20 ppm (m, 12H); ^{13}C NMR (100 MHz, $CDCl_3$): δ = 169.1, 166.0, 165.5, 161.0, 136.6, 134.8, 129.6, 129.3, 128.3, 127.6, 117.6, 116.9, 112.5, 111.0, 39.7, 33.1, 29.0, 28.7, 28.4, 28.1, 26.2, 11.7 ppm; ESI-HRMS calcd for $[C_{19}H_{24}N_2O_2S+H]^+$: 345.16313 *m*/*z*, found: 345.1638 *m*/*z*; HPLC purity: 98.1%.

(*Z*)-2-Mercapto-*N*-(7-(5-methyl-3-phenylisoxazol-4-yl)hept-6-enyl)acetamide (*cis*-13a): Compound *cis*-**13a** (65%) was prepared from *cis*-**25** according to the procedure described for **7a** (see Supporting Information scheme 2 for isolation of *cis*-**25**). ^{1}H NMR (400 MHz, $CDCl_3$): δ = 7.73 (m, 2H), 7.43 (m, 3H), 6.79 (s, 1H), 6.08 (d, *J* = 10.8 Hz, 1H), 5.77 (dt, *J* = 7.2 Hz, 11.2 Hz, 1H), 3.23–3.15 (m, 4H), 2.33 (s, 3H), 1.91 (q, *J* = 7.2 Hz, 2H), 1.85 (t, *J* = 8.8 Hz, 1H), 1.40 (m, 2H), 1.32 (m, 2H), 1.22 ppm (m, 2H); ^{13}C NMR (100 MHz, $CDCl_3$): δ = 170.1, 166.4, 161.3, 136.9, 129.8, 129.7, 128.8, 128.0, 117.3, 111.4, 40.1, 29.2, 29.0, 28.7, 28.3, 26.6, 12.0 ppm; ESI-HRMS calcd for $[C_{19}H_{24}N_2O_2S+H]^+$: 345.1631 *m*/*z*, found: 345.1628 *m*/*z*; HPLC purity: 98.5%.

(*E*)-2-Mercapto-*N*-(7-(5-methyl-3-phenylisoxazol-4-yl)hept-6-enyl)acetamide (*trans*-13a): Compound *trans*-**13a** (71%) was prepared from *trans*-**25** according to the procedure described for **7a** (see Supporting Information scheme 2 for isolation of *trans*-**25**). ^{1}H NMR (400 MHz, $CDCl_3$): δ = 7.63 (m, 2H), 7.45 (m, 3H), 6.78 (s, 1H), 6.07 (d, *J* = 16.0 Hz, 1H), 5.77 (dt, *J* = 6.8 Hz, 16.0 Hz, 1H), 3.31–3.06 (m, 4H), 2.48 (s, 3H), 2.17 (q, *J* = 7.2 Hz, 2H), 1.84 (t, *J* = 9.0 Hz, 1H), 1.57 (m, 2H), 1.48–1.34 ppm (m, 4H); ^{13}C NMR (100 MHz, $CDCl_3$): δ = 169.7, 165.8, 161.5, 135.1, 129.8, 129.6, 128.8, 128.7, 118.0, 112.8, 40.2, 33.4, 29.4, 29.1, 28.4, 26.6, 12.3 ppm; ESI-HRMS calcd for $[C_{19}H_{24}N_2O_2S+H]^+$: 345.1631 *m*/*z*, found: 345.1630 *m*/*z*; HPLC purity: 97.5%.

***N*-[7-(5-Methyl-3-phenylisoxazol-4-yl)hept-6-enyl]-2-mercaptopropionamide (13b)**: Compound **13b** *Z*/*E* 6:4 (18%) was prepared from compound **12** in three steps according to the methodology described for **4**, **6b**, and **7b**. ^{1}H NMR (400 MHz, $CDCl_3$): δ = 7.75–7.73 (m, 2H), 7.63–7.62 (m, 2H), 7.46–7.41 (m, 6H), 6.47 (br, 1H), 6.35 (br, 1H), 6.10–6.05 (m, 2H), 5.83–5.79 (m, 2H), 3.43–3.32 (m, 2H), 3.28–3.23 (m, 2H), 3.19–3.13 (m, 2H), 2.48 (s, 3H), 2.34 (s, 3H), 2.19–2.13 (m, 2H), 2.00–1.96 (m, 2H), 1.93–1.91 (m, 2H), 1.55–1.52 (m, 6H), 1.43–1.22 ppm (m, 12H); ^{13}C NMR (100 MHz, $CDCl_3$): δ = 172.6, 166.1, 165.6, 161.1, 136.7, 134.8, 129.8, 129.4, 128.6, 127.8, 117.8, 117.2, 112.6, 111.1, 39.7, 38.3, 33.2, 29.2, 28.8, 28.5, 26.3, 22.3, 11.9 ppm; ESI-HRMS calcd for $[C_{20}H_{26}N_2O_2S+H]^+$: 359.17878 *m*/*z*, found: 359.1785 *m*/*z*; HPLC purity: 97.4%.

***N*-[7-(5-Methyl-3-phenylisoxazol-4-yl)hept-6-enyl]-2-mercaptoisobutyramide (13c)**: Compound **13c** *Z*/*E* 7:3 (49%) was prepared from compound **12** in three steps according to the methodology described for **4**, **6c**, and **7c**. ^{1}H NMR (400 MHz, $CDCl_3$): δ = 7.74–7.72 (m, 2H), 7.62–7.60 (m, 2H), 7.44–7.40 (m, 6H), 6.97 (br, 1H), 6.86 (br, 1H), 6.08–6.04 (m, 2H), 5.83–5.77 (m, 2H), 3.24–3.21 (m, 2H), 3.16–3.11 (m, 2H), 2.46 (s, 3H), 2.32 (s, 3H), 2.17–2.13 (m, 2H), 1.92–1.90 (m, 2H), 1.56 (s, 12H), 1.42–1.21 ppm (m, 12H); ^{13}C NMR (100 MHz, $CDCl_3$): δ = 175.0, 166.1, 165.5, 161.0, 136.7, 134.8, 129.8, 129.4, 128.6, 127.8, 117.7, 117.1, 112.5, 111.1, 47.7, 39.9, 33.2, 30.3, 29.1, 28.8, 28.5, 26.3, 11.9 ppm; ESI-HRMS calcd for $[C_{21}H_{28}N_2O_2S+H]^+$: 371.17987 *m*/*z*, found: 371.1785 *m*/*z*; HPLC purity: 96.4%.

***N*-[7-(5-Methyl-3-phenylisoxazol-4-yl)hept-6-enyl]-2-pivaloylsulfanylacetamide (13d)**: Compound **13d** *Z*/*E* 7:3 (42%) was prepared from compound **12** in two steps according to the methodology described for **4** and **6d**. Purification of the obtained crude mixture was done using preparative HPLC Method B. ^{1}H NMR (400 MHz, $CDCl_3$): δ = 7.71–7.68 (m, 2H), 7.59–7.57 (m, 2H), 7.41–7.37 (m, 6H), 6.35 (br, 1H), 6.25 (br, 1H), 6.03–6.00 (m, 2H), 5.79–5.73 (m, 2H), 3.44 (s, 2H), 3.42 (s, 2H), 3.20–3.14 (m, 2H), 3.11–3.06 (m, 2H), 2.43 (s, 3H), 2.28 (s, 3H), 2.14–2.09 (m, 2H), 1.89–1.83 (m, 2H), 1.44–1.14 ppm (m, 30H); ^{13}C NMR (100 MHz, $CDCl_3$): δ = 206.8, 168.2, 165.9, 165.4, 160.9, 136.6, 134.8, 129.6, 129.2, 128.4, 127.6, 117.5, 116.9, 112.4, 111.0, 46.3, 39.4, 33.0, 32.3, 29.0, 28.7, 28.4, 27.0, 26.2, 11.7 ppm; ESI-HRMS calcd for $[C_{24}H_{32}N_2O_3S+H]^+$: 429.22064 *m*/*z*, found: 429.2185 *m*/*z*; HPLC purity: 98.4%.

(*Z*)-(*S*)-2-(7-(5-Methyl-3-phenylisoxazol-4-yl)hept-6-enylamino)-2-oxoethyl 2,2-dimethylpropanethioate (*cis*-13d): Compound *cis*-**13d** was isolated from **13d** by chiral column chromatography. ^{1}H NMR (400 MHz, $CDCl_3$): δ = 7.71 (m, 2H), 7.41 (m, 3H), 6.16 (s, 1H), 6.06 (d, *J* = 10.8 Hz, 1H), 5.79 (m, 1H), 3.44 (s, 2H), 3.12 (q, *J* = 6.8 Hz, 2H), 2.32 (s, 3H), 1.89 (q, *J* = 7.2 Hz, 2H),1.37–1.27 (m, 4H), 1.25–1.15 ppm (m, 11H); ^{13}C NMR (100 MHz, $CDCl_3$): δ = 207.3, 168.6, 166.3, 161.3, 136.9, 129.9, 129.6, 128.7, 128.0, 117.3, 111.3, 46.7, 39.7, 32.7, 29.3, 29.1, 28.8, 27.4, 26.5, 12.0 ppm; ESI-HRMS calcd for $[C_{24}H_{32}N_2O_3S+H]^+$: 429.2206 *m*/*z*, found: 429.2217 *m*/*z*; HPLC purity: 99.8%.

(*E*)-(*S*)-2-(7-(5-Methyl-3-phenylisoxazol-4-yl)hept-6-enylamino)-2-oxoethyl 2,2-dimethylpropanethioate (*trans*-13d): Compound *trans*-**13d** was isolated from **13d** by chiral column chromatography. ^{1}H NMR (400 MHz, $CDCl_3$): δ = 7.62 (m, 2H), 7.45 (m, 3H), 6.20 (s, 1H), 6.06 (d, *J* = 16.0 Hz, 1H), 5.76 (dt, *J* = 7.0 Hz, 16.0 Hz, 1H), 3.47 (s, 2H), 3.21 (q, *J* = 6.8 Hz, 2H), 2.48 (s, 3H), 2.15 (q, *J* = 7.2 Hz, 2H), 1.49 (m, 4H), 1.33 (m, 2H), 1.25 ppm (s, 9H); ^{13}C NMR (100 MHz, $CDCl_3$): δ = 207.5, 168.7, 165.8, 161.5, 135.1, 129.9, 129.6, 128.8, 128.7, 118.0, 112.8, 46.8, 39.8, 33.5, 32.7, 29.5, 29.1, 27.5, 26.5, 12.3 ppm; ESI-HRMS calcd for $[C_{24}H_{32}N_2O_3S+H]^+$: 429.2206 *m*/*z*, found: 429.2212 *m*/*z*; HPLC purity: 99.4%.

***tert*-Butyl 5-(5-methyl-3-phenylisoxazol-4-ylmethoxy)pentylcarbamate (14)**: The alcohol **10** (190 mg, 1 mmol), PPh_3 (315 mg, 1.2 mmol), and imidazole (88 mg, 1.3 mmol) were dissolved in anhydrous CH_2Cl_2 (5 mL) under Ar atmosphere. I_2 (305 mg, 1.2 mmol) was added in one portion to the flask through a temporarily opened neck at 0 °C. The mixture was stirred at room temperature for 3 h. After evaporating the solvent, the residue was purified by a short column (SiO_2, EtOAc/hexanes 70:30) to remove baseline impurities and to obtain the crude intermediate 4-(iodomethyl)-5-methyl-3-phenylisoxazole. NaH (60 mg, 1.5 mmol) was added in one portion to a solution of 5-(Boc-amino)-1-pentanol (305 mg,

 © 2012 Wiley-VCH Verlag GmbH & Co. KGaA, Weinheim

1.5 mmol) in dry DMF (5 mL) at 0 °C. The mixture was cooled to −20 °C; then a solution of the crude compound 4-(iodomethyl)-5-methyl-3-phenylisoxazole in anhydrous DMF (5 mL) was added slowly. The mixture was warmed to room temperature and stirred overnight. After quenching with a saturated NH_4Cl solution (10 mL), the mixture was extracted with EtOAc. The organic layer was washed with H_2O and brine and dried over Na_2SO_4. The solvent was removed in vacuo, and the residue was purified by column chromatography (SiO_2, EtOAc/hexanes 75:25→50:50) to afford the title product **14** (112 mg, 30%) as a colorless oil. ^{1}H NMR (400 MHz, $CDCl_3$): δ = 7.78–7.75 (m, 2H), 7.46–7.43 (m, 3H), 4.31 (s, 2H), 3.45 (t, J = 6.4 Hz, 2H), 3.09–3.08 (m, 2H), 2.48 (s, 3H), 1.63–1.58 (m, 2H), 1.49–1.33 ppm (m, 13H); ^{13}C NMR (100 MHz, $CDCl_3$): δ = 168.8, 167.2, 162.7, 129.5, 129.2, 128.7, 128.3, 110.5, 70.0, 61.5, 40.2, 29.8, 29.2, 28.4, 24.0, 11.2 ppm.

(*R*)-*N*-{5-[(5-Methyl-3-phenylisoxazol-4-yl)methoxy]pentyl}-2-(tritylthio)propanamide ((*R*)-15): Compound (*R*)-**15** was isolated from a racemic mixture of compound **15** using chiral column chromatography. Compound **15** was prepared from **14** according to the methodology described for **4** and **6b**. ^{1}H NMR (400 MHz, $CDCl_3$): δ = 7.79 (m, 2H), 7.47 (m, 9H), 7.25 (m, 9H), 4.33 (s, 2H), 3.45 (t, J = 6.4 Hz, 2H), 2.97 (m, 2H), 2.69 (m, 1H), 2.50 (s, 3H), 1.57 (m, 2H), 1.46 (d, J = 7.5 Hz, 3H), 1.29 ppm (m, 4H); ^{13}C NMR (100 MHz, $CDCl_3$): δ = 172.2, 168.9, 162.7, 144.3, 129.6, 129.4, 129.3, 128.7, 128.3, 128.1, 127.0, 110.6, 69.9, 68.1, 61.5, 44.6, 39.6, 29.3, 28.9, 23.6, 20.2, 11.3 ppm; $[\alpha]_D^{20}$ = +36.0 (c = 0.2, $CHCl_3$).

(*S*)-*N*-{5-[(5-Methyl-3-phenylisoxazol-4-yl)methoxy]pentyl}-2-(tritylthio)propanamide ((*S*)-15): Compound (*S*)-**15** was isolated from a racemic mixture of compound **15** using chiral column chromatography. Compound **15** was prepared from **14** according to the methodology described for **4** and **6b**. ^{1}H NMR (400 MHz, $CDCl_3$): δ = 7.79 (m, 2H), 7.45 (m, 9H), 7.26 (m, 9H), 4.32 (s, 2H), 3.45 (t, J = 6.3 Hz, 2H), 2.97 (m, 2H), 2.72 (m, 1H), 2.49 (s, 3H), 1.58 (m, 2H), 1.45 (d, J = 7.5 Hz, 3H), 1.29 ppm (m, 4H); ^{13}C NMR (100 MHz, $CDCl_3$): δ = 172.2, 168.8, 162.7, 144.3, 129.6, 129.4, 129.2, 128.7, 128.3, 128.1, 127.0, 110.6, 69.9, 68.1, 61.5, 44.5, 39.6, 29.3, 28.9, 23.6, 20.2, 11.3 ppm; $[\alpha]_D^{20}$ = −27.0 (c = 0.4, $CHCl_3$).

2-Mercapto-*N*-[5-(5-methyl-3-phenylisoxazol-4-ylmethoxy)pentyl]propionamide (16): Compound **16** (32%) was prepared from compound **14** in three steps according to the methodologies described for **4**, **6b**, and **7b**. ^{1}H NMR (400 MHz, $CDCl_3$): δ = 7.78–7.76 (m, 2H), 7.47–7.44 (m, 3H), 6.45 (br, 1H), 4.32 (s, 2H), 3.46 (t, J = 6.4 Hz, 2H), 3.43–3.35 (m, 1H), 3.26–3.21 (m, 2H), 2.49 (s, 3H), 1.98 (d, J = 8.4 Hz, 1H), 1.65–1.60 (m, 2H), 1.56–1.49 (m, 5H), 1.43–1.37 ppm (m, 2H); ^{13}C NMR (100 MHz, $CDCl_3$): δ = 172.7, 168.8, 162.7, 129.6, 129.3, 128.7, 128.3, 110.6, 69.9, 61.5, 39.8, 38.3, 29.3, 29.2, 23.6, 22.3, 11.3 ppm; ESI-HRMS calcd for $[C_{19}H_{26}N_2O_3S+H]^+$: 363.17369 m/z, found: 363.1740 m/z; HPLC purity: 99.4%.

(*R*)-2-Mercapto-*N*-{5-[(5-methyl-3-phenylisoxazol-4-yl)methoxy]pentyl}propanamide ((*R*)-16): Compound (*R*)-**16** (56%) was prepared from compound (*R*)-**15** according to the methodology described for **7a**. ^{1}H NMR (400 MHz, $CDCl_3$): δ = 7.77 (m, 2H), 7.45 (m, 3H), 6.55 (s, 1H), 4.32 (s, 2H), 3.48–3.38 (m, 3H), 3.24 (q, J = 6.8 Hz, 2H), 2.48 (s, 3H), 1.99 (d, J = 8.0 Hz, 1H), 1.63 (m, 2H), 1.51 (m, 5H), 1.40 ppm (m, 2H); ^{13}C NMR (100 MHz, $CDCl_3$): δ = 173.3, 169.1, 162.9, 129.9, 129.4, 129.0, 128.5, 110.8, 70.1, 61.7, 40.0, 38.5, 29.4, 29.3, 23.8, 22.4, 11.5 ppm; $[\alpha]_D^{20}$ = +15.0 (c = 0.09, $CHCl_3$); ESI-HRMS calcd for $[C_{19}H_{26}N_2O_3S+H]^+$: 363.1737 m/z, found: 363.1729 m/z; HPLC purity: 98.7%.

(*S*)-2-Mercapto-*N*-{5-[(5-methyl-3-phenylisoxazol-4-yl)methoxy]pentyl}propanamide ((*S*)-16): Compound (*S*)-**16** (56%) was prepared from compound (*S*)-**15** according to the methodology described for **7a**. ^{1}H NMR (400 MHz, $CDCl_3$): δ = 7.78 (m, 2H), 7.45 (m, 3H), 6.51 (s, 1H), 4.32 (s, 2H), 3.48–3.40 (m, 3H), 3.24 (q, J = 6.8 Hz, 2H), 2.49 (s, 3H), 1.99 (d, J = 8.0 Hz, 1H), 1.64 (m, 2H), 1.52 (m, 5H), 1.40 ppm (m, 2H); ^{13}C NMR (100 MHz, $CDCl_3$): δ = 173.2, 169.1, 163.0, 129.9, 129.4, 129.0, 128.5, 110.8, 70.1, 61.7, 40.0, 38.5, 29.5, 29.4, 23.9, 22.5, 11.5 ppm; $[\alpha]_D^{20}$ = −13.6 (c = 0.08, $CHCl_3$); ESI-HRMS calcd for $[C_{19}H_{26}N_2O_3S+H]^+$: 363.1737 m/z, found: 363.1728 m/z; HPLC purity: 96.4%.

5-(3-Fluorophenyl)-4-iodo-3-methylisoxazole (17b): *n*-Butyllithium (9.4 mL, 15 mmol) was slowly added to 1-ethynyl-3-fluorobenzene (1.15 mL, 10 mmol) in THF (50 mL) at −78 °C. The reaction mixture was stirred at 0 °C for 30 min, then cooled to −78 °C. $ZnCl_2$ (2 g, 15 mmol) in THF (15 mL) and then acetyl chloride (1.42 mL) were added. The reaction mixture was stirred at room temperature for 1 h and quenched with hexanes (10 mL). The organic layer was washed with brine (15 mL) and dried over anhydrous Na_2SO_4. Purification of the crude reaction mixture by column chromatography (SiO_2, 0→20% EtOAc/hexanes) afforded 4-(3-fluorophenyl)-but-3-yn-2-one (1.6 g, 98%) as a pale-yellow oil. ^{1}H NMR (400 MHz, $CDCl_3$): δ = 7.38–7.16 (m, 4H), 2.47 ppm (s, 3H); ^{13}C NMR (100 MHz, $CDCl_3$): δ = 184.2, 163.4, 160.9, 130.3, 128.8, 121.6, 119.7, 119.4, 118.2, 118.0, 88.4, 88.2, 32.6 ppm.

NH_2OH·HCl (1.67 g, 20 mmol) and pyridine (2.83 mL, 35 mmol) were added to this ketone in CH_3OH (30 mL) with Na_2SO_4 (2.84 g, 20 mmol). The reaction mixture was stirred at reflux for 17 h and then the volatiles were evaporated. The crude mixture was dissolved in EtOAc, washed with H_2O, washed with brine, and dried over anhydrous Na_2SO_4 to afford the racemic 4-(3-fluorophenyl)-but-3-yn-2-one *O*-methyloxime (1.6 g, 85%) as a yellow oil. ^{1}H NMR (400 MHz, $CDCl_3$): δ = 7.48–7.03 (m, 8H), 3.96 (s, 3H), 3.95 (s, 3H), 2.10 (s, 3H), 2.06 ppm (s, 3H); ^{13}C NMR (100 MHz, $CDCl_3$): δ = 163.4, 161.0, 149.8, 130.0, 127.8, 123.7, 118.7, 118.5, 116.6, 116.3, 97.4, 88.6, 62.5, 62.3, 20.9, 20.4 ppm.

To this oxime in CH_2Cl_2 (60 mL) was added 1 M ICl in CH_2Cl_2 (10.2 mL, 10.2 mmol). The reaction mixture was stirred at room temperature overnight, and saturated $Na_2S_2O_3$ was added. The aqueous layer was extracted with CH_2Cl_2 (3×30 mL). The combined organic layers were dried over anhydrous Na_2SO_4. Purification of the crude reaction mixture by preparative HPLC Method A afforded the title compound (526 mg, 41%) as a yellow oil. ^{1}H NMR (400 MHz, $CDCl_3$): δ = 7.81–7.79 (m, 1H), 7.73–7.71 (m, 1H), 7.45–7.39 (m, 1H), 7.16–7.11 (m, 1H), 2.31 ppm (s, 3H); ^{13}C NMR (100 MHz, $CDCl_3$): δ = 165.6, 163.6, 163.0, 161.2, 130.3, 128.8, 122.7, 117.4, 117.2, 114.1, 113.9, 58.6, 12.4 ppm.

2-Mercapto-*N*-[7-(3-methyl-5-phenylisoxazol-4-yl)hept-6-ynyl]propionamide (18a): To the 4-iodo-3-methyl-5-phenylisoxazole **17a** (1 g, 3.5 mmol) in DMF (16 mL) was added *tert*-butyl hept-6-ynylcarbamate (1.48 g, 7 mmol) [generated from 6-heptynenitrile by reduction of the nitrile with $LiAlH_4$ in Et_2O and Boc protection of the obtained amine], $PdCl_2(PPh_3)_2$ (245 mg, 0.35 mmol), CuI (133 mg, 0.7 mmol) and DIEA (16 mL). The reaction mixture was irradiated at 130 °C for 20 min. EtOAc (30 mL) was added. The organic layer was washed with H_2O (3×50 mL) and dried over anhydrous Na_2SO_4. Purification of the crude reaction mixture by column chromatography (SiO_2, 0→100% EtOAc/hexanes) afforded *tert*-butyl 7-(3-methyl-5-phenylisoxazol-4-yl)hept-6-ynylcarbamate (0.87 g, 67%) as a yellow oil. ^{1}H NMR (400 MHz, $CDCl_3$): δ = 8.12–8.09 (m, 2H), 7.49–7.43 (m, 3H), 4.53 (s, 1H), 3.14–3.13 (m, 2H), 2.51 (t, J = 6.4 Hz, 2H), 2.34 (s, 3H), 1.70–1.63 (m, 2H), 1.53–1.49 (m, 4H), 1.43 ppm (s, 9H); ^{13}C NMR (100 MHz, $CDCl_3$): δ = 167.6, 162.0, 155.9, 130.2,

 © 2012 Wiley-VCH Verlag GmbH & Co. KGaA, Weinheim

128.7, 127.4, 125.9, 99.5, 97.2, 79.1, 70.0, 40.4, 29.6, 28.4, 28.2, 26.0, 19.6, 10.5 ppm.

The Boc protecting group was removed according to the methodology described for **4** to afford 7-(3-methyl-5-phenylisoxazol-4-yl)hept-6-ynylamine TFA salt. ^{1}H NMR (400 MHz, CD_3OD): δ = 8.09–8.07 (m, 2H), 7.50–7.48 (m, 3H), 2.95–2.89 (m, 2H), 2.57 (t, J = 6.4 Hz, 2H), 2.30 (s, 3H), 1.75–1.68 (m, 4H), 1.62–1.55 ppm (m, 2H); ^{13}C NMR (100 MHz, CD_3OD): δ = 168.9, 163.3, 161.0, 131.7, 130.0, 128.5, 126.9, 100.6, 98.6, 70.7, 40.6, 29.2, 28.1, 26.8, 20.0, 10.4 ppm.

***N*-[7-(3-Methyl-5-phenylisoxazol-4-yl)hept-6-ynyl]-2-tritylsulfanylpropionamide** (43%) was prepared from the obtained amine according to the methodology described for **6b**. ^{1}H NMR (400 MHz, $CDCl_3$): δ = 8.12–8.10 (m, 2H), 7.49–7.43 (m, 9H), 7.29–7.26 (m, 6H), 7.22–7.18 (m, 3H), 5.99 (br, 1H), 3.05–2.97 (m, 2H), 2.76–2.71 (m, 1H), 2.50–2.46 (m, 2H), 2.33 (s, 3H), 1.63–1.58 (m, 2H), 1.44 (d, J = 7.2 Hz, 3H), 1.39–1.33 ppm (m, 4H); ^{13}C NMR (100 MHz, $CDCl_3$): δ = 172.0, 167.4, 161.8, 144.1, 130.1, 129.2, 128.5, 127.9, 127.3, 126.8, 125.7, 99.3, 97.0, 69.9, 67.9, 44.3, 39.4, 28.4, 28.0, 25.9, 20.0, 19.4, 10.4 ppm.

Compound 18a (79%) was prepared from the obtained propionamide according to the methodology described for **7a**. ^{1}H NMR (400 MHz, $CDCl_3$): δ = 8.07–8.05 (m, 2H), 7.45–7.39 (m, 3H), 6.70 (br, 1H), 3.40–3.33 (m, 1H), 3.26–3.21 (m, 2H), 2.47 (t, J = 6.8 Hz, 2H), 2.29 (s, 3H), 1.99 (d, J = 8.4 Hz, 1H), 1.67–1.60 (m, 2H), 1.58–1.47 ppm (m, 7H); ^{13}C NMR (100 MHz, $CDCl_3$): δ = 172.9, 167.4, 161.8, 130.2, 128.5, 127.1, 125.7, 99.3, 97.1, 69.8, 39.5, 37.9, 28.8, 28.0, 25.9, 22.1, 19.4, 10.3 ppm; ESI-HRMS calcd for $[C_{20}H_{24}N_2O_2S+H]^+$: 357.16313 *m/z*, found: 357.1638 *m/z*; HPLC purity: 98.9%.

7-[5-(3-Fluorophenyl)-3-methylisoxazol-4-yl]hept-6-ynyl-2-mercaptopropionamide (18b): Compound **18b** (20%) was prepared from compound **17b** in four steps according to the methodology described for **18a**. ^{1}H NMR (400 MHz, $CDCl_3$): δ = 7.83–7.79 (m, 2H), 7.42–7.36 (m, 1H), 7.11–7.06 (m, 1H), 6.67 (br, 1H), 3.39–3.34 (m, 1H), 3.27–3.22 (m, 2H), 2.48 (t, J = 6.8 Hz, 2H), 2.29 (s, 3H), 1.99 (d, J = 8.0 Hz, 1H), 1.68–1.61 (m, 2H), 1.58–1.47 ppm (m, 7H); ^{13}C NMR (100 MHz, $CDCl_3$): δ = 172.8, 166.0, 163.7, 161.9, 161.3, 130.3, 129.0, 121.4, 117.1, 116.9, 112.7, 112.5, 100.2, 98.0, 69.6, 39.5, 37.9, 28.8, 28.0, 26.0, 22.1, 19.4, 10.3 ppm; ESI-HRMS calcd for $[C_{20}H_{23}FN_2O_2S+H]^+$: 375.15370 *m/z*, found: 375.1540 *m/z*; HPLC purity: 99.4%.

2-Mercapto-2-methyl-*N*-[7-(3-methyl-5-phenylisoxazol-4-yl)hept-6-ynyl]propionamide (18c): Compound **18c** (24%) was prepared using compound **5c** in four steps according to the methodology described for **18a**. ^{1}H NMR (400 MHz, $CDCl_3$): δ = 8.12–8.10 (m, 2H), 7.49–7.43 (m, 3H), 6.96 (br, 1H), 3.29–3.24 (m, 2H), 2.52 (t, J = 6.8 Hz, 2H), 2.34 (s, 3H), 2.11 (s, 1H), 1.71–1.66 (m, 2H), 1.62–1.51 ppm (m, 10H); ^{13}C NMR (100 MHz, $CDCl_3$): δ = 175.0, 167.6, 162.0, 130.3, 128.7, 127.4, 125.9, 99.5, 97.1, 70.1, 47.8, 39.9, 30.4, 29.0, 28.2, 26.1, 19.6, 10.5 ppm; ESI-HRMS calcd for $[C_{21}H_{26}N_2O_2S+H]^+$: 371.17878 *m/z*, found: 371.1784 *m/z*; HPLC purity: 96.2%.

2-Mercapto-2-methyl-*N*-[6-(3-methyl-5-phenylisoxazol-4-yl)hex-5-ynyl]propionamide (18d): Compound **18d** (30%) was prepared with *tert*-butyl hex-5-ynylcarbamate and compound **5c** in four steps according to the methodology described for **18a**. ^{1}H NMR (400 MHz, $CDCl_3$): δ = 8.07–8.05 (m, 2H), 7.45–7.37 (m, 3H), 7.02 (br, 1H), 3.31–3.26 (m, 2H), 2.52 (t, J = 6.8 Hz, 2H), 2.30 (s, 3H), 2.15 (s, 1H), 1.70–1.64 (m, 4H), 1.55 ppm (s, 6H); ^{13}C NMR (100 MHz, $CDCl_3$): δ = 175.0, 167.5, 161.8, 130.2, 128.6, 127.2, 125.8, 99.3, 96.7, 70.2, 47.5, 39.3, 30.2, 28.6, 25.8, 19.2, 10.4 ppm; ESI-HRMS calcd for $[C_{20}H_{24}N_2O_2S+H]^+$: 357.16313 *m/z*, found: 357.1636 *m/z*; HPLC purity: 98.3%.

***N*-[6-(3-Methyl-5-phenylisoxazol-4-yl)hex-5-ynyl]-2-pivaloylsulfanylacetamide (18e)**: Compound **18e** (16%) was prepared with *tert*-butyl hex-5-ynylcarbamate and compound **5d** in three steps according to the methodology described for **18a**. ^{1}H NMR (400 MHz, $CDCl_3$): δ = 8.10–8.08 (m, 2H), 7.49–7.44 (m, 3H), 6.42 (br, 1H), 3.51 (s, 2H), 3.33–3.28 (m, 2H), 2.52 (t, J = 6.8 Hz, 2H), 2.33 (s, 3H), 1.70–1.62 (m, 4H), 1.22 ppm (s, 9H); ^{13}C NMR (100 MHz, $CDCl_3$): δ = 207.4, 169.4, 167.7, 162.0, 130.3, 128.7, 127.3, 125.9, 99.4, 96.6, 70.3, 46.5, 39.2, 32.3, 28.5, 27.2, 25.7, 19.3, 10.5 ppm; ESI-HRMS calcd for $[C_{23}H_{28}N_2O_3S+H]^+$: 413.18934 *m/z*, found: 413.1898 *m/z*; HPLC purity: 99.6%.

***tert*-Butyl 4-[*trans*-2-(3-methyl-5-phenylisoxazol-4-yl)vinyl]benzylcarbamate (19)**: *tert*-Butyl 4-vinylbenzylcarbamate (327 mg, 1.4 mmol) [generated from Boc-protection of 4-vinylbenzylamine], $Pd(OAc)_2$ (16 mg, 0.07 mmol), nBu$_4$NCl (194 mg, 0.7 mmol), and Na_2CO_3 (148 mg, 1.4 mmol) were added to 4-iodo-3-methyl-5-phenylisoxazole (0.2 g, 0.7 mmol) in DMF (3 mL). The reaction mixture was irradiated at 130 °C for 1 h. EtOAc was added. The organic layer was washed with H_2O (3×20 mL) and dried over anhydrous Na_2SO_4 to afford the title compound (180 mg, 66%) as a brown oil. ^{1}H NMR (400 MHz, $CDCl_3$): δ = 7.71–7.68 (m, 2H), 7.48–7.43 (m, 3H), 7.40–7.38 (m, 2H), 7.30–7.26 (m, 2H), 6.95 (d, J = 16.4 Hz, 1H), 6.85 (d, J = 16.4 Hz, 1H), 5.28 (s, 1H), 4.31–4.29 (m, 2H), 2.46 (s, 3H), 1.48 ppm (s, 9H); ^{13}C NMR (100 MHz, $CDCl_3$): δ = 165.2, 158.6, 155.8, 138.8, 135.7, 131.3, 129.6, 128.6, 127.8, 127.5, 127.2, 126.2, 116.4, 112.6, 79.1, 44.0, 28.1, 11.8 ppm.

2-Mercapto-*N*-(4-[*trans*-2-(3-methyl-5-phenylisoxazol-4-yl)vinyl]-benzyl)propionamide (20a): Compound **20a** (10%) was prepared from compound **19** in three steps according to the methodologies described for **4**, **6b**, and **7b**. ^{1}H NMR (400 MHz, $CDCl_3$): δ = 7.74–7.72 (m, 2H), 7.52–7.46 (m, 3H), 7.44–7.42 (m, 2H), 7.30–7.26 (m, 2H), 6.99 (d, J = 16.8 Hz, 1H), 6.89 (d, J = 16.8 Hz, 1H), 6.80 (br, 1H), 4.47–4.45 (m, 2H), 3.51–3.47 (m, 1H), 2.50 (s, 3H), 2.05 (d, J = 8.4 Hz, 1H), 1.60 ppm (d, J = 8.4 Hz, 3H); ^{13}C NMR (100 MHz, $CDCl_3$): δ = 172.7, 165.8, 158.9, 135.7, 136.4, 131.3, 130.0, 128.9, 128.1, 127.5, 126.2, 117.2, 112.8, 43.6, 38.2, 22.2, 12.1 ppm; ESI-HRMS calcd for $[C_{22}H_{22}N_2O_2S+H]^+$: 379.14748 *m/z*, found: 379.1477 *m/z*; HPLC purity: 96.9%.

2-Mercapto-2-methyl-*N*-(4-[*trans*-2-(3-methyl-5-phenylisoxazol-4-yl)vinyl]benzyl)propionamide (20b): Compound **20b** (55%) was prepared from compound **19** in three steps according to the methodologies described for **4**, **6c**, and **7c**. ^{1}H NMR (400 MHz, $CDCl_3$): δ = 7.72–7.69 (m, 2H), 7.50–7.45 (m, 3H), 7.43–7.41 (m, 2H), 7.35 (br, 1H), 7.28–7.26 (m, 2H), 6.97 (d, J = 16.4 Hz, 1H), 6.87 (d, J = 16.4 Hz, 1H), 4.45–4.43 (m, 2H), 2.47 (s, 3H), 2.26 (s, 1H), 1.64 ppm (s, 6H); ^{13}C NMR (100 MHz, $CDCl_3$): δ = 174.9, 165.4, 158.7, 138.0, 136.0, 131.3, 129.8, 127.8, 127.3, 126.0, 116.8, 112.7, 47.3, 43.5, 30.2, 11.9 ppm; ESI-HRMS calcd for $[C_{23}H_{24}N_2O_2S+H]^+$: 393.16313 *m/z*, found: 393.1624 *m/z*; HPLC purity: 99.0%.

HDAC isoform inhibition

HDAC inhibition assays were performed by the Reaction Biology Corporation (Malvern, PA) using human full-length recombinant HDAC1, 2, 5, and 6 isolated from a baculovirus expression system in Sf9 cells. A complex of human full-length recombinant HDAC3 co-expressed with human NCOR2 was used in the HDAC3 assays, and residues 627–1085 of human recombinant HDAC4 were used for the HDAC4 assays. An acetylated, fluorogenic peptide derived from residues 379–382 of p53 ($RHKK_{Ac}$) was used as the substrate in the assays. The reaction buffer contained 50 mM Tris·HCl pH 8.0, 137 mM NaCl, 2.7 mM KCl, 1 mM $MgCl_2$, 1 mg mL^{-1} BSA, and a final

 © 2012 Wiley-VCH Verlag GmbH & Co. KGaA, Weinheim

concentration of 1% DMSO. The enzyme was delivered into wells of the reaction plate and compounds were delivered in 100% DMSO into the enzyme mixture by Acoustic technology (Echo550 instrument; nanoliter range). The plates were spun down and pre-incubated for 5–10 min. The substrate was then delivered to all reaction wells to initiate the reaction, which was incubated for 2 h at 30 °C. After incubation, developer and TSA were added to quench the reaction and generate fluorescence. Kinetic measurements were then taken for 1.5 h at 15-min intervals to ensure that development was complete. Endpoint readings were taken for analysis after the development reached a plateau. Dose–response curves were generated, and the IC_{50} value for each compound was extrapolated from the generated plots (ten-dose IC_{50} curves were generated using a threefold serial dilution pattern starting at 30 μM).

Molecular modeling

The two enantiomers (*R*)-**7b** and (*S*)-**7b** were simulated considering the thiol function in its anionic form. The conformational behavior of these compounds was investigated using a Monte Carlo procedure (as implemented in the VEGA suite of programs, http://www.vegazz.net/), which generated 1000 conformers by randomly rotating the rotors. All geometries so obtained were stored and optimized to avoid high-energy rotamers. The 1000 conformers were clustered according to their similarity in order to discard redundancies; in this analysis, two geometries were considered non-redundant when they differed by $>60°$ in at least one torsion angle. For each ligand, the so obtained lowest-energy structure was then exploited in the following docking simulations.

As mentioned above, the resolved structures of HDAC2 and HDAC4 were retrieved from the RCSB PDB, while the homology model of the HDAC6 subtype had been recently generated by us.[14] The experimental structures were completed by adding hydrogen atoms; the side chains of Arg, Lys, Glu, and Asp were ionized to remain compatible with physiological pH values, while His residues were considered neutral by default apart from those belonging to cited dyads, which are reported in Supporting Information table 1. In particular, in all docking simulations, only the first histidine residue (His145, His158, and His610 for HDAC2, 4, and 6, respectively) was protonated. In all simulated HDAC structures, the second neutral histidine (His146, His159, and His611 for HDAC2, 4, and 6, respectively) was considered in its N^{ε} tautomeric form in order to minimize steric hindrance within the catalytic pocket. The structures so obtained were minimized while keeping the backbone fixed to preserve the experimental folding for HDAC2 and 4 and the predicted folding of HDAC6.

Docking simulations were performed by *GriDock*, a parallel tool based on the AutoDock 4.0 engine.[37] In detail, the grid box was set to include all residues within a 15 Å radius around the catalytic metal ion, thus comprising the entire catalytic cavity. The resolution of the grid was $60\times60\times60$ points with a grid spacing of 0.450 Å. Each inhibitor was docked into this grid with the Lamarckian algorithm as implemented in AutoDock. For the docking simulations, the flexible bonds of the ligand were automatically recognized by *GriDock* and left free to rotate. The genetic-based algorithm ran 20 simulations per substrate with 2×10^6 energy evaluations and a maximum number of generations set to 27000. The crossover rate was increased to 0.8, and the number of individuals in each population to 150. All other parameters were left at the AutoDock default settings. The docking results were ranked considering both AutoDock scores and the distance between the zinc ion and sulfur atom. The best complexes were minimized keeping all atoms outside of a 15 Å radius around the bound substrate fixed to favor the mutual adaptability between the ligand and enzyme. The optimized complexes were then used to re-calculate the AutoDock docking scores and VEGA energy scores.

Mercaptoacetamide dimerization

These experiments were performed on a Shimadzu LC–MS 2010EV Liquid Chromatograph Mass Spectrometer. Electrospray ionization was used in positive mode with a scan range of 300–800 *m/z* with scans occurring every 0.5 s. A Halo C_8 3.0×30 mm column with 2.7 μm particle size was used at a flow rate of 0.2 mL min^{-1}; gradient: 25% CH_3CN/H_2O to 100% CH_3CN, 8 min; 100% CH_3CN, 2 min; 100% CH_3CN to 25% CH_3CN/H_2O, 0.1 min; 25% CH_3CN/H_2O, 49.9 min. LC–MS solvents were purchased from commercial sources and each contained 0.1% formic acid. Each compound (100 μg) was dissolved in 1 mL CH_3OH, and 1 μL aliquots were analyzed every hour for 24 h. Normalized peaks corresponding to the $[M+H]^+$ and $[M+Na]^+$ ions for both the monomer and dimer were extracted from the total ion chromatogram (TIC), and the area under each respective peak in the extracted ion chromatograms (XIC) was calculated using the automatic integration feature available in Shimadzu's LCMS Solutions software (Columbia, MD, USA). The cutoff for peak width was set at 20 s, and the rest of the parameters were left at default settings. The ratio of total dimer to total monomer was calculated by adding the areas of the $[M+H]^+$ and $[M+Na]^+$ peaks for each respectively and calculating the quotient. The ratio was then plotted against time for each compound.

Neuroprotection and glutathione depletion

For the neuroprotection studies, cells were rinsed with warm PBS and then placed in minimum essential medium (Invitrogen) containing 5.5 g L^{-1} glucose, 10% fetal calf serum, 2 mM L-glutamine, and 100 μM cysteine. Oxidative stress was induced by the addition of the cysteine homologue, homocysteine (HCA; 5 mM), to the media. HCA was diluted from 100-fold concentrated solutions that were adjusted to pH 7.5. In combination with HCA, the novel HDAC inhibitors (10 μM) were added. Viability was assessed after 48 h by calcein-acetoxymethyl ester (AM)/ethidium homodimer-1 staining (live/dead assay; Molecular Probes, Eugene, OR, USA) using fluorescence microscopy and the MTT assay (3-(4,5-dimethylthiazol-2-yl)-2,5-diphenyltetrazolium bromide) method.

Total intracellular glutathione (GSH + GSSG) measurements of primary neuron cultures were determined with the GSH-Glo Glutathione Assay kit (Promega) according to the manufacturer's protocol. Primary cortical neurons were plated at 1×10^5 cells per well in a poly-D-lysine-coated 96-well plate. After incubation for 24 h, neurons were exposed to HCA in the presence or absence of drug for 8 h. Neurons were lysed with DTT containing lysis buffer to convert any GSSG to GSH, allowing the determination of total GSH. The lysates were incubated with a reaction buffer containing the luciferin precursor luciferin-NT and the enzyme GST. In the presence of GSH, GST converts luciferin-NT into luciferin. A subsequent reaction buffer containing the enzyme luciferase, which produces light as a by-product of luciferin metabolism, was added to the lysates, and the light intensity (which correlates with GSH levels) was measured with a luminometer (LMax II 384, Molecular Devices). The values were normalized to protein concentration as determined by a Bradford protein assay. GSH standards were used to calculate GSH concentrations.

 © 2012 Wiley-VCH Verlag GmbH & Co. KGaA, Weinheim

Acknowledgements

The authors thank Dr. Brett Langley and Kathryn McLaughlin at Burke Medical Research Institute for performing the neuroprotection and glutathione depletion studies. The authors also thank the Alzheimer's Drug Discovery Foundation (grant no. 271210) for supporting this work.

Keywords: dimerization · enantioselectivity · histone deacetylases · mercaptoacetamides · neurological agents

[1] M. Dokmanovic, C. Clarke, P. A. Marks, *Mol. Cancer Res.* **2007**, *5*, 981 – 989.
[2] J. Wu, M. Grunstein, *Trends Biochem. Sci.* **2000**, *25*, 619 – 623.
[3] E. Verdin, F. Dequiedt, H. G. Kasler, *Trends Genet.* **2003**, *19*, 286 – 293.
[4] R. B. Parmigiani, W. S. Xu, G. Venta-Perez, H. Erdjument-Bromage, M. Yaneva, P. Tempst, P. A. Marks, *Proc. Natl. Acad. Sci. USA* **2008**, *105*, 9633 – 9638.
[5] J. J. Kovacs, P. J. Murphy, S. Gaillard, X. Zhao, J. T. Wu, C. V. Nicchitta, M. Yoshida, D. O. Toft, W. B. Pratt, T. P. Yao, *Mol. Cell* **2005**, *18*, 601 – 607.
[6] X. Wu, P. S. Chen, S. Dallas, B. Wilson, M. L. Block, C. C. Wang, H. Kinyamu, N. Lu, X. Gao, Y. Leng, D. M. Chuang, W. Zhang, R. B. Lu, J. S. Hong, *Int. J. Neuropsychopharmacol.* **2008**, *11*, 1123 – 1134.
[7] J. P. Dompierre, J. D. Godin, B. C. Charrin, F. P. Cordelieres, S. J. King, S. Humbert, F. Saudou, *J. Neurosci.* **2007**, *27*, 3571 – 3583.
[8] K. Ververis, T. C. Karagiannis, *Am. J. Transl. Res.* **2011**, *3*, 454 – 467.
[9] Y. Zhang, S. Kwon, T. Yamaguchi, F. Cubizolles, S. Rousseaux, M. Kneissel, C. Cao, N. Li, H. L. Cheng, K. Chua, D. Lombard, A. Mizeracki, G. Matthias, F. W. Alt, S. Khochbin, P. Matthias, *Mol. Cell Biol.* **2008**, *28*, 1688 – 1701.
[10] T. Suzuki, N. Miyata, *Curr. Med. Chem.* **2005**, *12*, 2867 – 2880.
[11] Y. Kawaguchi, J. J. Kovacs, A. McLaurin, J. M. Vance, A. Ito, T. P. Yao, *Cell* **2003**, *115*, 727 – 738.
[12] K. V. Butler, A. P. Kozikowski, *Curr. Pharm. Des.* **2008**, *14*, 505 – 528.
[13] J. E. Bradner, N. West, M. L. Grachan, E. F. Greenberg, S. J. Haggarty, T. Warnow, R. Mazitschek, *Nat. Chem. Biol.* **2010**, *6*, 238 – 243.
[14] K. V. Butler, J. Kalin, C. Brochier, G. Vistoli, B. Langley, A. P. Kozikowski, *J. Am. Chem. Soc.* **2010**, *132*, 10842 – 10846.
[15] A. P. Kozikowski, Y. Chen, A. Gaysin, B. Chen, M. A. D'Annibale, C. M. Suto, B. C. Langley, *J. Med. Chem.* **2007**, *50*, 3054 – 3061.
[16] R. Konsoula, M. Jung, *Int. J. Pharm.* **2008**, *361*, 19 – 25.
[17] M. Whittaker, C. D. Floyd, P. Brown, A. J. Gearing, *Chem. Rev.* **1999**, *99*, 2735 – 2776.
[18] W. K. Kelly, O. A. O'Connor, L. M. Krug, J. H. Chiao, M. Heaney, T. Curley, B. MacGregore-Cortelli, W. Tong, J. P. Secrist, L. Schwartz, S. Richardson, E. Chu, S. Olgac, P. A. Marks, H. Scher, V. M. Richon, *J. Clin. Oncol.* **2005**, *23*, 3923 – 3931.
[19] D. Kim, C. L. Frank, M. M. Dobbin, R. K. Tsunemoto, W. Tu, P. L. Peng, J. S. Guan, B. H. Lee, L. Y. Moy, P. Giusti, N. Broodie, R. Mazitschek, I. Delalle, S. J. Haggarty, R. L. Neve, Y. Lu, L. H. Tsai, *Neuron* **2008**, *60*, 803 – 817.
[20] M. A. Rivieccio, C. Brochier, D. E. Willis, B. A. Walker, M. A. D'Annibale, K. McLaughlin, A. Siddiq, A. P. Kozikowski, S. R. Jaffrey, J. L. Twiss, R. R. Ratan, B. Langley, *Proc. Natl. Acad. Sci. USA* **2009**, *106*, 19599 – 19604.
[21] N. Suzuki, T. Suzuki, Y. Ota, T. Nakano, M. Kurihara, H. Okuda, T. Yamori, H. Tsumoto, H. Nakagawa, N. Miyata, *J. Med. Chem.* **2009**, *52*, 2909 – 2922.
[22] S. K. Anandan, J. S. Ward, R. D. Brokx, M. R. Bray, D. V. Patel, X. X. Xiao, *Bioorg. Med. Chem. Lett.* **2005**, *15*, 1969 – 1972.
[23] J. E. Payne, C. Bonnefous, C. A. Hassig, K. T. Symons, X. Guo, P. M. Nguyen, T. Annable, P. L. Wash, T. Z. Hoffman, T. S. Rao, A. K. Shiau, J. W. Malecha, S. A. Noble, J. H. Hager, N. D. Smith, *Bioorg. Med. Chem. Lett.* **2008**, *18*, 6093 – 6096.
[24] R. Furumai, A. Matsuyama, N. Kobashi, K. H. Lee, M. Nishiyama, H. Nakajima, A. Tanaka, Y. Komatsu, N. Nishino, M. Yoshida, S. Horinouchi, *Cancer Res.* **2002**, *62*, 4916 – 4921.
[25] Y. M. Cui, J. Y. Li, L. L. Chen, J. Li, Q. Z. Ye, F. J. Nan, *Bioorg. Med. Chem.* **2004**, *12*, 2853 – 2861.
[26] C. Yan, Z. Xiu, X. Li, S. Li, C. Hao, H. Teng, *Proteins* **2008**, *73*, 134 – 149.
[27] C. A. Hassig, K. T. Symons, X. Guo, P. M. Nguyen, T. Annable, P. L. Wash, J. E. Payne, D. A. Jenkins, C. Bonnefous, C. Trotter, Y. Wang, J. V. Anzola, E. L. Milkova, T. Z. Hoffman, S. J. Dozier, B. M. Wiley, A. Saven, J. W. Malecha, R. L. Davis, J. Muhammad, A. K. Shiau, S. A. Noble, T. S. Rao, N. D. Smith, J. H. Hager, *Mol. Cancer Ther.* **2008**, *7*, 1054 – 1065.
[28] P. Bertrand, *Eur. J. Med. Chem.* **2010**, *45*, 2095 – 2116.
[29] R. Wu, Z. Lu, Z. Cao, Y. Zhang, *J. Am. Chem. Soc.* **2011**, *133*, 6110 – 6113.
[30] C. d'Ydewalle, J. Krishnan, D. M. Chiheb, P. Van Damme, J. Irobi, A. P. Kozikowski, P. V. Berghe, V. Timmerman, W. Robberecht, L. Van Den Bosch, *Nat. Med.* **2011**, *17*, 968 – 974.
[31] A. G. Kazantsev, L. M. Thompson, *Nat. Rev. Drug Discovery* **2008**, *7*, 854 – 868.
[32] Y. Ying, K. Taori, H. Kim, J. Hong, H. Luesch, *J. Am. Chem. Soc.* **2008**, *130*, 8455 – 8459.
[33] Y. Liu, L. A. Salvador, S. Byeon, Y. Ying, J. C. Kwan, B. K. Law, J. Hong, H. Luesch, *J. Pharmacol. Exp. Ther.* **2010**, *335*, 351 – 361.
[34] A. Bowers, N. West, J. Taunton, S. L. Schreiber, J. E. Bradner, R. M. Williams, *J. Am. Chem. Soc.* **2008**, *130*, 11219 – 11222.
[35] W. Chen, R. Hartman, R. Ayer, S. Marcantonio, J. Kamper, J. Tang, J. H. Zhang, *J. Neurochem.* **2009**, *111*, 726 – 736.
[36] W. K. Kelly, P. A. Marks, *Nat. Clin. Pract. Oncol.* **2005**, *2*, 150 – 157.
[37] G. Vistoli, A. Pedretti, A. Mazzolari, B. Testa, *J. Comput. Aided Mol. Des.* **2010**, *24*, 771 – 787.

Received: November 11, 2011
Revised: December 9, 2011
Published online on January 10, 2012

 © 2012 Wiley-VCH Verlag GmbH & Co. KGaA, Weinheim